IEEE Access
Multidisciplinary | Rapid Review | Open Access Journal

Received 30 July 2024, accepted 12 August 2024, date of publication 16 August 2024, date of current version 27 August 2024.

Digital Object Identifier 10.1109/ACCESS.2024.3444696

RESEARCH ARTICLE

Joint Beamforming and Power Allocation Design in Cooperative MIMO-NOMA Networks

ZAIN UL ABIDIN JAFFRI[1] AND MUHAMMAD FAHEEM[2], (Member, IEEE)
[1]School of International Education, International Scholarly Exchange Curriculum Program, Xiamen University of Technology, Xiamen 361024, China
[2]School of Technology and Innovations, University of Vaasa, 65200 Vaasa, Finland

Corresponding author: Muhammad Faheem (muhammad.faheem@uwasa.fi)

The work of Muhammad Faheem was supported in part by the Academy of Finland and the University of Vaasa, Finland.

ABSTRACT Due to its improved spectral efficiency, non-orthogonal multiple access (NOMA) is regarded as a promising multiple access technology for beyond fifth-generation (5G) networks. In this paper, we examine the performance of a cell-edge user and suggest a beamforming scheme in a cooperative two-user multiple-input multiple-output (MIMO)-NOMA system with Rayleigh fading channels. In the envisaged scenario, a cell-center user with better channel gain harvests energy and assists a cell-edge user with poorer channel conditions by using a simultaneous wireless information and power transfer mechanism. We first obtain the outage probability expressions in closed form for the cell-edge user for the Kronecker structured channel model in the covariance shaping and indefinite quadratic form. Next, the beamformers at the transmitter and receiver are introduced to reduce outage probability, with transmit beamformers maximizing the signal-to-leakage-plus-noise ratio and receive beamformers minimizing cross-covariance across all users. Furthermore, beamformers are adopted in the two-user network to adjust the power ratio and power allocation coefficients for better performance of the cell-edge user. Moreover, our scheme is also compared with a transmit antenna selection baseline scheme. Simulation results demonstrate that our approach enhances the performance of the two-user cooperative MIMO-NOMA system's performance, validating the theoretical analysis.

INDEX TERMS Relaying transmission, covariance shaping, Rayleigh quotient, optimization, outage probability.

I. INTRODUCTION

Due to the limited availability of wireless spectrum resources, spectrum efficiency and system capacity remain major issues for future generation mobile communication systems. By superposing users' signals in the same orthogonal resource, non-orthogonal multiple access (NOMA) is considered an effective mechanism to support high data rate medium access [1]. Specific technical implementations, like sparse code, power-domain NOMA, and pattern division multiple access are recommended by academia and industry to provide more user connectivity and higher spectral efficiency gain [2]. Although these technical implementations appear to have significant differences, their core concepts are the same. The basic principle of power-domain NOMA is to support users by using multiplexing at the transmitter and successive interference cancellation (SIC) at the receiver. As demonstrated by many studies, NOMA achieves better channel capacity and significantly outperforms orthogonal multiple access (OMA) schemes. Power domain NOMA [3] was the first proposed among all these technical implementations as a representative case. In addition, by using more antennas, multiple-input multiple-output (MIMO) could achieve high capacity [4]. Then a combination of NOMA and MIMO technologies can take advantage in both space and power domains, further enhancing system spectrum efficiency.

A. RELATED WORK

In this subsection, we elaborate on recent related work on NOMA, simultaneous wireless information and power

The associate editor coordinating the review of this manuscript and approving it for publication was Yunlong Cai.

transfer (SWIPT), and their applications to MIMO networks using covariance shaping and beamforming. For a NOMA multiuser downlink system, [5] presented a beamforming scheme based on zero-forcing and user pairing technique, assuming complete channel state information at the transmitter (CSIT). However, it is challenging to attain accurate instantaneous CSIT because of rapidly fading user channels or inadequate feedback. Hence, a statistical CSIT-based solution may be preferable in emerging systems, especially for mmWave and terahertz (THz) communications. In [6], the effect of partial CSIT on NOMA performance was studied by assuming a homogeneous distribution of users across a disc.

The influence of user grouping was studied in [7] where two different power distribution techniques were investigated. The first is NOMA with fixed power allocation (F-NOMA), whereas the second is NOMA inspired by cognitive radio (CR-NOMA). The power allocation problem in [8] was addressed in NOMA systems to achieve user fairness among users. This power allocation problem was further investigated in [9] with a modulation scheme in NOMA systems based on finite constellation sizes. SWIPT is a new concept that can help energy-constrained networks last longer and is regarded as an enabling technique for better connectivity of the Internet of things (IoT) for beyond fifth-generation (B5G) communications. The main idea of SWIPT, which was first proposed in [10], is to extract energy from information signals received. Due to practical constraints, it is difficult to decode information for a receiver while harvesting the energy. In [11], the SWIPT protocol was utilized in the NOMA system to analyze the far user performance. In [11], an equalizer and precoder design was developed for a two-user cooperative NOMA system in the existence of both inter-user interference and self-interference, where power allocation coefficients were updated using beamformers and a SWIPT protocol, and an exact outage probability expression was obtained. In [11], using the indefinite quadratic form (IQF) and the SWIPT protocol, the authors were able to obtain both approximate and exact outage probability expressions. MIMO has been utilized as a key enabler for future generation deployment [12]. Despite several well-studied benefits of MIMO, some challenges remain, most notably the channel vectors corresponding to each user having large dimensionality [13]. These issues arise as a result of the challenging implementation of large matrix operations in precoders/decoders, as well as from the overhead linked with pilot-assisted training and channel state feedback.

In response to these concerns, a couple of influential studies [14], [15] have highlighted the significance of statistical data in the MIMO regime. In this context, MIMO covariance shaping was used in [14] by introducing statistical beamforming to target channel statistics shaping performed at users. In particular, covariance shaping schemes using multiple antennas and the realistic non-Kronecker structure in MIMO channels were performed at the user side [15]. Feedback overhead was lowered by using the low-rank behaviour of channel covariance matrices [16]. Alternatively, while employing pilot sequences in the channel estimation step which were non-orthogonal [17] and in the precoding step [18], two distant user equipment (UE) with non-overlapping signal subspaces can be discriminated using statistical information only to mitigate interference. Furthermore, using second-order statistics, beamforming for both transmitter and receiver in a downlink system with multi-user MIMO was proposed in [19]. Outage probability was evaluated using an analytical expression for both the traditional Kronecker structured model and a generic channel model in [19] by utilizing a covariance shaping technique. The authors of [19] also proposed transmit and receive beamformer design in order to minimize outage probability.

Furthermore, a significant part of the literature focused on beamforming at the base station (BS), where it was separated into inner and outer precoding matrices [20], [21]. The former relies only on second-order channel statistics, whereas the latter depends on instantaneous CSI. As a consequence, the pilot length for instantaneous effective channel estimation is shortened, and the complexity of the inner precoding design is reduced [20]. Furthermore, in frequency-division duplex (FDD) systems, statistical CSI may be utilized to decrease the number of channels by taking advantage of the angle spreads' orthogonality of various user groups [22]. Existing work in time-division duplex (TDD) systems has shown how the application of statistical CSI allows for efficient pilot reuse across users [23]. Pilot reuse across spatially correlated Rayleigh fading channels for massive MIMO transmissions precoded using second-order channel statistics was discussed in [24], showing a decrease in the variance of the channel estimate error proportional to the number of antennas at the receiver. A channel estimating method was proposed in [25] to deal with circumstances where the angle spreads of the targeted and interfering channels overlap, utilizing statistical CSI to separate the channels [21]. A two-user cooperative MIMO-NOMA system, focusing on precoder and equalizer design for a cell-edge user, was proposed in [26]. They introduce a SWIPT-aided cooperative strategy that incorporates self-interference and beamforming, deriving a closed-form expression for the outage probability based on transmit correlation matrices. Their approach relies on channel modeling using transmit correlation matrices knowledge, neglecting the benefits of covariance shaping and potentially leading to issues in self-interference management.

The results of the existing research rely on a certain structure of the users' channel covariance matrices in terms of the degree of signal subspace separation and rank. The locations of the users with the scattering environment are the factors that are usually beyond the network designer's control. Indeed, when users are not sufficiently far apart, they show high spatial correlation in many practical scenarios. As a result, the requirement for signal subspaces that are orthogonal or non-overlapping is rarely met in reality [12].

Shaping the covariance matrix of the channel at the user side by exploiting the existing spatial selectivity features of users is referred to as covariance shaping. This is achieved through statistical beamforming, which essentially makes users evoke an appropriate subset of all possible directions of the BS for minimum spatial correlation.

Motivated by the above-mentioned work, the features of covariance shaping can be used for various purposes, including lowering the feedback overhead during the channel estimate phase and reducing interference during the downlink data transmission phase. To the best of our knowledge, the covariance shaping-based mechanism for MIMO-NOMA networks has not yet been investigated in depth. We have summarized the key features, advantages, and disadvantages of the related work in Table 1.

B. CONTRIBUTIONS

In this paper, we propose a cooperative two-user data transmission scheme using MIMO-NOMA, in which a near user (user-N) with strong channel gains uses the harvested energy obtained from the BS to forward messages to a far user (user-F) with weak channel conditions. The objective of this scheme is to improve the outage probability of user-F, formulated as a multi-objective optimization problem in a two-user MIMO-NOMA system. We employ a receive beamformer structure based on the generic Rayleigh quotient (G-RQ) using signal segmentation into non-overlapping subspaces and covariance shaping to address this problem. Our main contributions are summarized as follows:

- We propose the novel concept of MIMO-NOMA covariance shaping, aiming to design covariance matrices of users to separate their signal subspaces, which would otherwise overlap.
- We derive an exact closed-form expression for the outage probability of both users by formulating signal-to-interference-plus-noise ratio (SINR) expressions for direct and relaying transmissions, utilizing the IQF framework and Kronecker structured model.
- We suggest a generalized G-RQ based receive beamformer and transmit beamformer design using covariance shaping and signal-to-leakage-plus-noise ratio (SLNR), respectively, enabling the transmitter to optimize signal power to the intended receiver.
- To enhance coverage probability, we address the challenging problem of joint optimization of power allocation and power splitting control by transforming it into two subproblems and solving them iteratively using alternating optimization algorithms.

The remaining sections of the paper are structured as follows: Section II describes the system model and SINR formulation of direct and relaying transmission. Section III deduces the outage probability expressions for both users. Section IV discusses statistical beamformer design criteria and its optimization. Section V presents an iterative resource allocation scheme, while Section VI validates the system model through simulations. Comparison of our proposed work with some recent works is enlightened in Section VI. Finally, Section VIII concludes the paper.

II. SYSTEM MODEL

We consider a two-user MIMO-NOMA system for downlink transmission consisting of a BS, user-N, and user-F having M_{B}, M_{N} and M_{F} antennas, respectively, as shown in Fig. 1. Here, $\mathbf{H}_{\mathrm{N}}$ and $H_{\mathbf{F}}$ indicate channel gains from BS to user-N and user-F, respectively. Similarly, the channel vector from user-N to user-F is denoted by $\mathbf{H}_{\mathrm{NF}}$. Also, in our work, we consider Rayleigh fading channels with additive noise, where the correlation matrices are known. Specifically, we assume independent and identically distributed (i.i.d.) Rayleigh flat fading for all wireless links. Furthermore, additive white Gaussian noise (AWGN) $n_a(n)$ and $n_c(n)$ with zero mean and variances σ_{N}^2 of user-N, and σ_{F}^2 of user-F is considered in our system model. In addition, the channel gain is expressed as $E[|h_{xy}|^2] = \frac{\beta}{(d_{xy}/d_o)^{\epsilon}}$, where β represents power attenuation, ϵ represents path loss exponent, d_{xy} represents the distance between adjacent nodes, and d_o represents reference distance. Table 2 summarizes the important notations.

For downlink MIMO-NOMA transmission, relaying transmission is carried out in two stages using time switching/power splitting (TS/PS) mechanism, as depicted in Fig. 1. The first phase involves direct information transmission to users N and F, as well as energy harvesting at user N. The second stage involves cooperative relaying transfer from user-N to user-F. A time block T is divided into three sub-blocks. User-N harvests energy during the first time sub-block (αT duration) using a percentage of the input power (ρ). Information decoding at user-N occurs within the second sub-time block, and it makes use of the remaining $(1-\rho)$ fraction of power. The energy gathered by user-N is used for relaying in the third sub-time block. The time period of the second and third-time blocks is the same, i.e., $(1-\alpha)\frac{T}{2}$. The BS remains silent during the third time block, when user-N transmits data to user-F, i.e., the relaying stage, to avoid interference because the same frequency is utilized for both direct and relaying transmissions. To avoid interference, direct and relaying transmissions occur in two separate time blocks.

A. FIRST STAGE: DIRECT INFORMATION PHASE

The modulated data $\mathbf{x}(n)$ is delivered from the BS to both users after combining with precoder vectors $\mathbf{w}_{\mathrm{N}}$ and $\mathbf{w}_{\mathrm{F}}$, i.e.,

$$\mathbf{x}(n) = \mathbf{w}_{\mathrm{N}} s_{\mathrm{N}} + \mathbf{w}_{\mathrm{F}} s_{\mathrm{F}}, \tag{1}$$

where s_{N} and s_{F} are the message signal intended for user-N and user-F, respectively. The coefficients of power allocation for user-N and user-F are p_{N} and p_{F}, respectively, and they follow the NOMA principle, i.e., $p_{\mathrm{N}} + p_{\mathrm{F}} = 1$ where $0 < p_{\mathrm{N}} < p_{\mathrm{F}}$. Also, $||\mathbf{w}_{\mathrm{N}}||^2 = ||\mathbf{w}_{\mathrm{F}}||^2 = 1$.

TABLE 1. Summary of related schemes.

Reference	Key Features	Advantages	Drawbacks
[5]	Zero-forcing and CSIT user pairing beamforming scheme	Improved downlink performance through user pairing	Due to rapid fading, it is difficult to obtain accurate instantaneous CSIT
[6]	NOMA performance with partial CSIT and homogeneous user distribution	Statistical CSIT communication suitable for mmWave and THz	Assumes a homogeneous distribution of users, which may not be realistic
[7]	Grouping of users with fixed power allocation (F-NOMA) and cognitive radio (CR-NOMA)	Investigate the impact of user groups on performance	Dynamic network conditions may not be fully addressed
[8]	Fair Power Allocation for Users in NOMA Systems	Improve fairness among users	The complexity of power allocation problem
[9]	Power allocation with limited constellation sizes in NOMA	Improved modulation schemes to achieve better performance	Increased complexity in modulation and power allocation
[10]	Introducing SWIPT for energy-constrained networks	Extend network lifespan and improve IoT connectivity	Difficult to decode information while harvesting energy
[11]	Design of SWIPT protocol, interference equalizer, and precoder in NOMA	Analyze remote users' performance, reduce the outage probability	Complexity in managing inter-user and self-interference
[12]	Utilization of MIMO in next-generation deployment	Significantly improve network capacity and reliability	Challenges with large dimensionality of channel vectors
[14], [15]	MIMO statistical beamforming with covariance shaping	Reduce feedback overhead for channel statistics	Challenges with non-Kronecker structure implementation
[16]	Low-rank behavior of channel covariance matrices	Feedback overhead reduction	Ineffective handling of dynamic user environments
[17], [18]	UEs discrimination with non-overlapping signal subspaces	Utilizing statistical information to reduce interference	Assumes orthogonality which may not be practical in all scenarios
[19]	Beamforming of transmitter and receiver with covariance shaping	Reduces outage probability, supports Kronecker and generic models	Complex design for beamformers in addition to large computational overhead
[20], [21]	Separation of internal and external precoding matrices in BS	Reduces pilot length, lowers inner precoding complexity	Dependent on second-order channel statistics
[22]	Angle spreads' orthogonality in FDD systems	Reduces number of required channels	Complexity in managing angle spreads for different user groups
[23], [24]	Effective pilot reuse with statistical CSI in TDD systems	Reduces pilot overhead, enhances channel estimate accuracy	Needs spatially correlated Rayleigh fading channels
[25]	Channel estimation with overlapping angle spreads	Improves channel separation	High complexity in angle spread management
[26]	SWIPT-Aided Cooperative MIMO-NOMA	Improved Outage Performance	Neglects Covariance Shaping

1) AT USER-N

The message of user-N received is expressed as

$$y_{\mathrm{N}} = \mathbf{H}_{\mathrm{N}}\mathbf{w}_{\mathrm{N}}\sqrt{p_{\mathrm{N}}P_s}s_{\mathrm{N}} + \mathbf{H}_{\mathrm{N}}\mathbf{w}_{\mathrm{F}}\sqrt{p_{\mathrm{F}}P_s}s_{\mathrm{F}} + v_{\mathrm{aN}}, \quad (2)$$

in which the first term denotes the signal that user-N receives, the second term indicates the interference to user-N due to user-F, $v_{\mathrm{aN}} = \mathbf{r}_{\mathrm{N}}\mathbf{n}_{\mathrm{aN}}$ where $\mathbf{n}_{\mathrm{aN}}$ is a noise vector of zero-mean and the maximum transmission power from the BS is Ps. Furthermore, we consider that the elements of $\mathbf{H}_{\mathrm{N}}$ satisfy $\mathrm{vec}(\mathbf{H}_{\mathrm{N}}) \sim \mathcal{CN}(0, \Sigma_{\mathrm{N}})$ [27]. The channel covariance matrix $\Sigma_{\mathrm{N}} \in \mathbb{C}^{M_{\mathrm{N}} \times M_{\mathrm{B}}}$ is expressed as

$$\Sigma_{\mathrm{N}} = \begin{bmatrix} \Sigma_{\mathrm{N}}^{(1,1)} & \cdots & \Sigma_{\mathrm{N}}^{(1,M_{\mathrm{B}})} \\ \vdots & \ddots & \vdots \\ \Sigma_{\mathrm{N}}^{(M_{\mathrm{B}},1)} & \cdots & \Sigma_{\mathrm{N}}^{(M_{\mathrm{B}},M_{\mathrm{B}})} \end{bmatrix}. \quad (3)$$

Here, the postscript (x, y) signifies the BS's y^{th} antenna element towards user-N's xth antenna element, and $\Sigma_{\mathrm{N}}^{x,y} \triangleq \mathbb{E}[\mathbf{h}_{\mathrm{N},x}\mathbf{h}_{\mathrm{N},y}^{H}] \in \mathbb{C}^{M_{\mathrm{N}} \times M_{\mathrm{N}}}$ depicts the matrix of cross covariance between xth and yth coloumns of $\mathbf{H}_{\mathrm{N}}$.

As user-N assists user-F, the energy (E_{N}) harvested by association with channel $\mathbf{H}_{\mathrm{N}}$ utilizing the hybrid TS/PS protocol is expressed as

$$E_{\mathrm{N}} = \eta P_s ||\mathbf{H}_{\mathrm{N}}\mathbf{w}_{\mathrm{N}}||^2 \alpha T + \eta\rho P_s ||\mathbf{H}_{\mathrm{N}}\mathbf{w}_{\mathrm{N}}||^2 (1-\alpha)T/2, \quad (4)$$

where η is the coefficient of energy efficiency in a range of $0 < \eta < 1$, which is utilized to decode data.
user-N receives, which is estimated at the receiver as

$$\hat{y}_{\mathrm{N}} = \sqrt{1-\rho} \left[\mathbf{r}_{\mathrm{N}}\mathbf{H}_{\mathrm{N}}\mathbf{w}_{\mathrm{N}}\sqrt{p_{\mathrm{N}}P_s}s_{\mathrm{N}} + \mathbf{r}_{\mathrm{N}}\mathbf{H}_{\mathrm{N}}\mathbf{w}_{\mathrm{F}}\sqrt{p_{\mathrm{F}}P_s}s_{\mathrm{F}} + v_{\mathrm{aN}}\right] + v_{\mathrm{cN}}, \quad (5)$$

where $\mathbf{r}_{\mathrm{N}}$ is the equalization vector having a length of $1 \times M_{\mathrm{N}}$ at user-N and $v_{\mathrm{cN}} = \mathbf{r}_{\mathrm{N}}\mathbf{n}_{\mathrm{cN}}$.

According to the principle of NOMA, at user-N after decoding user-F's message, a SIC receiver decodes its own message, i.e., s_{N}, from the received signal by removing the decoded message. By using NOMA and SIC, it may serve multiple users with the same time and same frequency

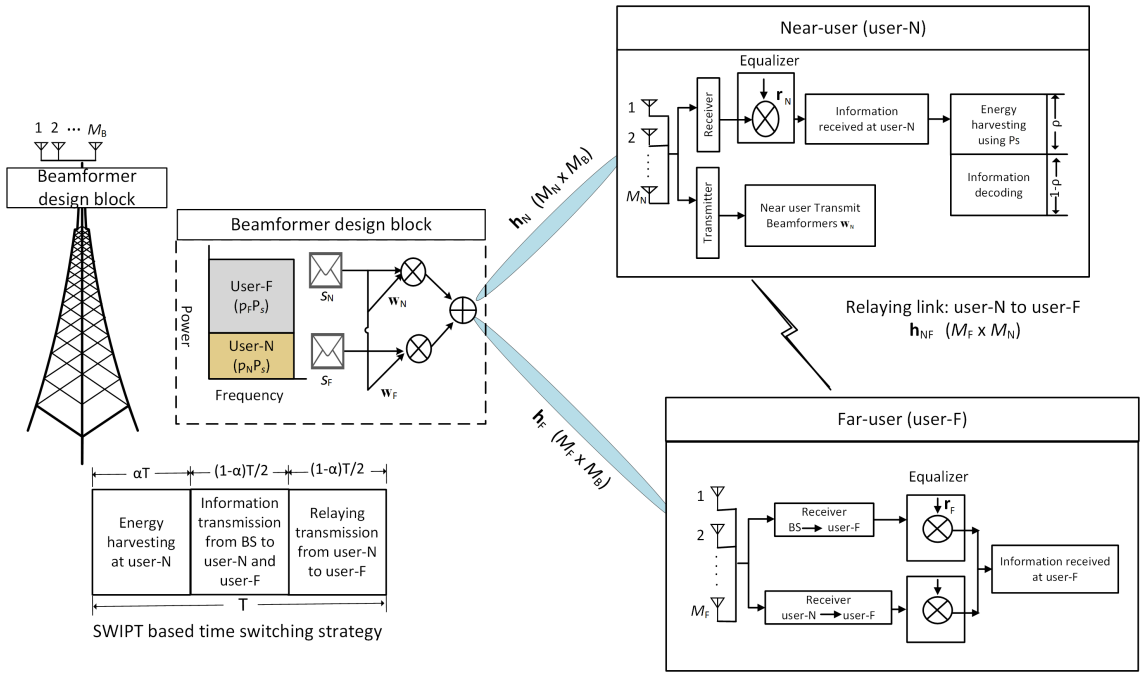

FIGURE 1. System model of a cooperative MIMO-NOMA system.

TABLE 2. List of notations.

Parameters	Descriptions
α	Fraction of time
β	Power attenuation
ρ	Fraction of power
η	Efficiency for energy conversion
γ_{th}	SNR threshold to decode the message $\Gamma_{\text{N}}^{s_{\text{F}}}$ correctly
$\Gamma_{\text{N}}^{s_{\text{F}}}$	SNR at user-N to decode s_{F}
$\Gamma_{\text{N}}^{s_{\text{N}}}$	SNR at user-N for self-message decoding s_{N}
Σ	Covariance matrix
d_o	Reference distance
d_{xy}	Distance between adjacent nodes
$\mathbf{H}$	Channel matrix
M_{B}	Antennas on base station
M_{N}, M_{F}	Antennas at user-N and user-F
$\mathcal{O}_{\text{N}}$	user-N's outage probability
$\mathcal{O}_{\text{F}}$	user-F's outage probability
P_s	Total transmit power from the BS
p_{N}, p_{F}	Coefficients for power allocation
$\mathbf{R}_{Nj-Tx}$, $\mathbf{R}_{Nj-Rx}$	Correlation matrices at transmitter and receiver
$\mathbf{r}_{\text{N}}$, $\mathbf{r}_{\text{F}}$, $\mathbf{r}_{\text{NF}}$	Equalizer vectors on the users
s_{N} , s_{F}	Information messages
$\mathbf{v}_{\text{N}}$, $\mathbf{v}_{\text{F}}$	Antenna noise power densities
$\mathbf{w}_{\text{N}}$, $\mathbf{w}_{\text{F}}$	Transmit beamformers

resources to achieve greater spectral efficiency while also reducing interference through SIC. As a result, the relevant SINR to decode s_{F} at user-N, denoted for brevity as $\Gamma_{\text{N}}^{s_{\text{F}}}$, is written as

$$\Gamma_{\text{N}}^{s_{\text{F}}} = \frac{|\mathbf{r}_{\text{N}}\mathbf{H}_{\text{N}}\mathbf{w}_{\text{B}}|^2(1-\rho)p_{\text{F}}P_s}{|\mathbf{r}_{\text{N}}\mathbf{H}_{\text{N}}\mathbf{w}_{\text{B}}|^2(1-\rho)p_{\text{N}}P_s + (1-\rho)\sigma_{\text{aN}}^2|\mathbf{r}_{\text{N}}\mathbf{v}_{\text{N}}|^2 + \sigma_{\text{cN}}^2}, \tag{6}$$

where user-N uses the received power portion ρ to harvest the energy and the remaining portion (1)-ρ) to decode the informations, where $0 < \rho < 1$ signifies the ratio of power-splitting. Next, we propose utilizing a generic channel model using covariance shaping [27] to convert (6) to a canonical form. The covariance shaping purpose is to get the orthogonal covariance matrices received by each user so that the interference can be minimized between the beams. The effective MIMO channel between the BS and users is given by $\tilde{\mathbf{h}}_{\text{N}} \triangleq \mathbf{r}_{\text{N}}\mathbf{H}_{\text{N}}$ implying $\tilde{\mathbf{h}}_{\text{N}} \sim \mathcal{CN}(0, \Psi_{\text{N}})$, where $\Psi_{\text{N}} \in \mathbb{C}^{M\times M}$ is the matrix of effective covariance computed as

$$\Psi_{\text{N}} = \left(\left(\mathbf{I}_M \bigotimes \mathbf{r}_{\text{N}}\right)\Sigma_{\text{N}}\left(\mathbf{I}_M \bigotimes \mathbf{r}_{\text{N}}^H\right)\right)^T. \tag{7}$$

Keeping the downlink transmission in focus, the SINR in (6) can be obtained using the notion of quadratic form[1] as,

$$\Gamma_{\text{N}}^{s_{\text{F}}} = \frac{(1-\rho)p_{\text{F}}P_s||\bar{\mathbf{h}}_{\text{N}}||^2_{\tilde{\mathbf{P}}_{\text{N}}}}{(1-\rho)p_{\text{N}}P_s||\bar{\mathbf{h}}_{\text{N}}||^2_{\tilde{\mathbf{P}}_{\text{N}}} + (1-\rho)\sigma_{\text{aN}}^2\text{tr}(\tilde{\mathbf{r}}_{\text{N}}^H\mathbf{r}_{\text{N}}) + \sigma_{\text{cN}}^2}, \tag{8}$$

where $\bar{\mathbf{h}}_{\text{N}} \triangleq \Psi_{\text{N}}^{\frac{-H}{2}}\tilde{\mathbf{h}}_{\text{N}}$. The antenna arrays at the transmission side and receiver side are assumed to be independent of each other. By using a Kronecker-based stochastic model (KBSM) [28], we can write $\Sigma_{\text{N}} = \left(\mathbf{R}_{\text{N}j-Tx}^T \bigotimes \mathbf{R}_{\text{N}j-Rx}\right)$, where $\mathbf{R}_{\text{N}j-Tx}$ and $\mathbf{R}_{\text{N}j-Rx}$ are the transmit and receive correlation matrices, respectively for user-N. Moreover, in (8), the

[1]The quadratic form for any vector $\mathbf{x}$ and matrix $\mathbf{A}$ is expressed as, $||x||^2 = x^HAx$.

subscripts P_N and $\tilde{P}_N$ denote two distinct matrices used respectively in the numerator and denominator to compute the norm of $\bar{h}_N$. We utilize the quadratic form in the whitened version, i.e., by relation [29]. The matrices $\mathbf{P}_\mathrm{N}$ and $\tilde{\mathbf{P}}_\mathrm{N}$ are defined as: $\mathbf{P}_\mathrm{N} = (\tilde{\mathbf{r}}_\mathrm{N} \bigotimes \tilde{\mathbf{w}}_\mathrm{N})^H(\tilde{\mathbf{r}}_\mathrm{N} \bigotimes \tilde{\mathbf{w}}_\mathrm{N})$ and $\tilde{\mathbf{P}}_\mathrm{N} = (\tilde{\mathbf{r}}_\mathrm{N} \bigotimes \tilde{\mathbf{w}}_\mathrm{F})^H(\tilde{\mathbf{r}}_\mathrm{N} \bigotimes \tilde{\mathbf{w}}_\mathrm{F})$, where $\bigotimes$ is the Kronecker product operator. Furthermore, the transmit and receive beamformers are obtained as $\tilde{\mathbf{w}}_\mathrm{N} = \mathbf{R}^{\frac{1}{2}}_{\mathrm{N}j-Tx}\mathbf{w}_\mathrm{N}$, and $\tilde{\mathbf{r}}_\mathrm{N} = \mathbf{R}_{\mathrm{N}j-Rx}\mathbf{R}^{\frac{1}{2}}_{\mathrm{N}j-Rx}$, respectively. Additionally, the effective MIMO channel $\tilde{\mathbf{h}}_\mathrm{F}$, representing the channel between the Base Station (BS) and user-F, is defined as $\tilde{\mathbf{h}}_\mathrm{F} \triangleq \mathbf{r}_\mathrm{F}\mathbf{H}_\mathrm{F}$, where $\tilde{\mathbf{h}}_\mathrm{F}$ follows a complex normal distribution $\mathcal{CN}(0, \Psi_\mathrm{F})$. Moreover, $\bar{\mathbf{h}}_\mathrm{N}$ which is defined as $\Psi_\mathrm{N}^{\frac{-H}{2}}\tilde{\mathbf{h}}_\mathrm{N}$, indicating the effective MIMO channel for $\bar{h}_N$. By considering these definitions, the norms of $\bar{h}_N$ with respect to the matrices $\mathbf{P}_\mathrm{N}$ and $\tilde{\mathbf{P}}_\mathrm{N}$ are calculated accordingly within (8).

Next, in order to decode user-N's message, the respective SINR i.e., $\Gamma_\mathrm{N}^{s_\mathrm{N}}$, is formulated as

$$\Gamma_\mathrm{N}^{s_\mathrm{N}} = \frac{(1-\rho)p_\mathrm{N}P_s||\bar{\mathbf{h}}_\mathrm{N}||^2_{\mathbf{P}_\mathrm{N}}}{(1-\rho)\sigma^2_{\mathrm{aN}}\mathrm{tr}(\tilde{\mathbf{r}}^H_\mathrm{N}\,\mathbf{R}_{\mathrm{N}j-Rx}) + \sigma^2_{\mathrm{cN}}}, \tag{9}$$

having no interference at user-N while decoding own user-N's message because of incorporation of SIC.

2) AT USER-F

The information signal that user-F receives is expressed as

$$y_F = \mathbf{H}_\mathrm{F}\mathbf{w}_\mathrm{N}\mathbf{r}_\mathrm{F}\sqrt{p_\mathrm{N}P_s}s_\mathrm{N} + \mathbf{H}_\mathrm{F}\mathbf{w}_\mathrm{F}\mathbf{r}_\mathrm{F}\sqrt{p_\mathrm{F}P_s}s_\mathrm{F} + \mathbf{r}_\mathrm{F}\mathbf{v}_\mathrm{F}(n). \tag{10}$$

Here, matrix $\mathbf{H}_\mathrm{F}$ is the channel matrix from BS to user-F and the interference due to user-N at user-F is considered as noise. The covariance matrix associated with channel $\mathbf{H}_\mathrm{F}$ is obtained by using the same procedure as in (3), and hence it is obtained as

$$\Sigma_\mathrm{F} = \begin{bmatrix} \Sigma_\mathrm{F}^{(1,1)} & \cdots & \Sigma_\mathrm{F}^{(1,M_\mathrm{B})} \\ \vdots & \ddots & \vdots \\ \Sigma_\mathrm{F}^{(M_\mathrm{B},1)} & \cdots & \Sigma_\mathrm{F}^{(M_\mathrm{B},M_\mathrm{B})} \end{bmatrix}, \tag{11}$$

where $\Sigma_\mathrm{F}^{x,y} \triangleq \mathbb{E}[\mathbf{h}_{\mathrm{F},x}\mathbf{h}^H_{\mathrm{F},y}] \in \mathbb{C}^{N\times N}$ represents the cross covariance matrix between the xth and yth coloumns of $\mathbf{H}_\mathrm{F}$.

As a result, the message s_F of user-F is decoded, the respective SINR ($\Gamma_\mathrm{F}^{s_\mathrm{F}}$), is given by

$$\Gamma_\mathrm{F}^{s_\mathrm{F}} = \frac{|\mathbf{r}_\mathrm{F}\mathbf{H}_\mathrm{F}\mathbf{w}_\mathrm{F}|^2 p_\mathrm{F}P_s}{|\mathbf{r}_\mathrm{F}\mathbf{H}_\mathrm{F}\mathbf{w}_\mathrm{N}|^2 p_\mathrm{N}P_s + |\mathbf{r}_\mathrm{F}\mathbf{v}_\mathrm{F}|^2}. \tag{12}$$

The effective MIMO channel $\tilde{\mathbf{h}}_\mathrm{F} \triangleq \mathbf{r}_\mathrm{F}\mathbf{H}_\mathrm{F}$ between the BS and user-F is implied as $\tilde{\mathbf{h}}_\mathrm{F} \sim \mathcal{CN}(0, \Psi_\mathrm{F})$, where $\Psi_\mathrm{F} \in \mathbb{C}^{M_\mathrm{F}\times M_\mathrm{F}}$ is the effective covariance matrix defined as $\Psi_\mathrm{F} = \left(\left(\mathbf{I}_M \bigotimes \mathbf{r}_\mathrm{F}\right)\Sigma_\mathrm{F}\left(\mathbf{I}_M \bigotimes \mathbf{r}^H_\mathrm{F}\right)\right)^T$.

Now, the SINR expression in (12) is presented in a canonical quadratic form as

$$\Gamma_\mathrm{F}^{s_\mathrm{F}} = \frac{p_\mathrm{F}P_s||\bar{\mathbf{h}}_\mathrm{F}||^2_{\mathbf{P}_\mathrm{F}}}{p_\mathrm{N}P_s||\bar{\mathbf{h}}_\mathrm{F}||^2_{\tilde{\mathbf{P}}_\mathrm{F}} + \sigma^2_\mathrm{F}\mathrm{tr}(\tilde{\mathbf{r}}^H_\mathrm{F}\,\mathbf{r}_\mathrm{F})}, \tag{13}$$

where $\bar{\mathbf{h}}_\mathrm{F} \triangleq \Psi_\mathrm{F}^{\frac{-H}{2}}\tilde{\mathbf{h}}_\mathrm{F}$. Here, again utilizing the KBSM, the correlation matrices at transmitter and receiver for user-F are $\mathbf{R}_{\mathrm{F}j-Tx}$ and $\mathbf{R}_{\mathrm{F}j-Rx}$, respectively, and hence $\Sigma_\mathrm{F} = \left(\mathbf{R}^T_{\mathrm{F}j-Tx} \bigotimes \mathbf{R}_{\mathrm{F}j-Rx}\right)$. We obtain $\mathbf{P}_\mathrm{F} = (\tilde{\mathbf{r}}_\mathrm{F} \bigotimes \tilde{\mathbf{w}}_\mathrm{F})^H(\tilde{\mathbf{r}}_\mathrm{F} \bigotimes \tilde{\mathbf{w}}_\mathrm{F})$, and $\tilde{\mathbf{P}}_\mathrm{F} = (\tilde{\mathbf{r}}_\mathrm{F} \bigotimes \tilde{\mathbf{w}}_\mathrm{N})^H(\tilde{\mathbf{r}}_\mathrm{F} \bigotimes \tilde{\mathbf{w}}_\mathrm{N})$. Furthermore, $\tilde{\mathbf{w}}_\mathrm{F} = \mathbf{R}^{\frac{1}{2}}_{\mathrm{F}j-Tx}\mathbf{w}_\mathrm{F}$, and $\tilde{\mathbf{r}}_\mathrm{F} = \mathbf{r}_\mathrm{F}\mathbf{R}^{\frac{1}{2}}_{\mathrm{F}j-Rx}$.

B. SECOND STAGE: RELAYING TRANSMISSION PHASE

The information is forwarded using the energy gathered in the first stage from user-N to user-F. The amount of power that user-N sends out for relaying process (as in [30]) is given as

$$\begin{aligned} p_\mathrm{N} &= \frac{E_\mathrm{N}}{(1-\alpha)T/2} \\ &= \frac{||\mathbf{h}_\mathrm{N}||^2_{\mathbf{P}_\mathrm{N}}(\eta P_s\alpha T + \eta\rho P_s(1-\alpha)T/2)}{(1-\alpha)T/2}, \end{aligned} \tag{14}$$

where (4) is used to obtain the second equality.

After the relaying operation, the message received at user-F from user-N is expressed as

$$y_\mathrm{NF} = \mathbf{r}_\mathrm{NF}\sqrt{p_\mathrm{N}}\widehat{s_\mathrm{F}}h_\mathrm{NF}\mathbf{w}_\mathrm{N} + \mathbf{r}_\mathrm{NF}\mathbf{v}_\mathrm{NF}(n), \tag{15}$$

where $\widehat{s_\mathrm{F}}$ is the version that has been re-encoded of s_F, while the covariance matrix at user-F from user-N is obtained as

$$\Sigma_\mathrm{NF} = \begin{bmatrix} \Sigma_\mathrm{NF}^{(1,1)} & \cdots & \Sigma_\mathrm{NF}^{(1,N)} \\ \vdots & \ddots & \vdots \\ \Sigma_\mathrm{NF}^{(N,1)} & \cdots & \Sigma_\mathrm{NF}^{(N,N)} \end{bmatrix}, \tag{16}$$

where $\Sigma_{\mathrm{NF},xy} \triangleq \mathbb{E}[\mathbf{h}_{\mathrm{NF},x}\mathbf{h}^H_{\mathrm{NF},y}] \in \mathbb{C}^{N\times N}$ indicates the cross covariance matrix between the xth and yth coloumns of $\mathbf{H}_\mathrm{NF}$. The effective channel between user-N and user-F is given by $\tilde{\mathbf{h}}_\mathrm{NF} \triangleq \mathbf{r}_\mathrm{NF}\mathbf{H}_\mathrm{NF}$ implying $\tilde{\mathbf{h}}_\mathrm{NF} \sim \mathcal{CN}(0, \Psi_\mathrm{NF})$, where $\Psi_\mathrm{NF} \in \mathbb{C}^{M_\mathrm{F}\times M_\mathrm{F}}$ is the effective covariance matrix defined as $\Psi_\mathrm{NF} = \left(\left(\mathbf{I}_M \bigotimes \mathbf{r}_\mathrm{NF}\right)\Sigma_\mathrm{NF}\left(\mathbf{I}_M \bigotimes \mathbf{r}^H_\mathrm{NF}\right)\right)^T$.

Furthermore, by using (14) and (15), the signal-to-noise ratio (SNR) from user-N to user-F in the context of detecting s_F is given by

$$\Gamma_\mathrm{NF} = \frac{|h_\mathrm{NF}|^2||\mathbf{h}_\mathrm{N}||^2_{\mathbf{P}_\mathrm{N}}\eta P_s(2\alpha + (1-\alpha)\rho)}{(\sigma^2_\mathrm{F} + \sigma^2_\mathrm{NF})(1-\alpha)}, \tag{17}$$

where $\sigma^2_\mathrm{F} + \sigma^2_\mathrm{NF}$ is the variance at user-F.

Finally, a selection combining (SC) is utilized to integrate the two information signals, namely the direct information signal and relaying information signal at user-F. Therefore, after integrating the two received signals, the achievable SNR at user-F is given by [30], [31], and [32]

$$\Gamma_\mathrm{F}^{\mathrm{SC}} = \max\left(\Gamma_\mathrm{NF}, \Gamma_\mathrm{F}^{s_\mathrm{F}}\right), \tag{18}$$

which implies that, if $\Gamma_\mathrm{F}^{s_\mathrm{F}} \gg \Gamma_\mathrm{NF}$, no relay is needed.

III. CHARACTERIZATION OF OUTAGE PROBABILITY FOR JOINT-PRECODING VECTORS

In this section, the outage probability, i.e., the probability of a user experiencing an instantaneous SINR below a predefined threshold is characterized for user-F and user-N.

A. OUTAGE PROBABILITY OF USER-F

Considering the beamformers $\mathbf{w}_{\mathrm{N}}$ and $\mathbf{w}_{\mathrm{F}}$ to be linearly dependent, the outage probability expression of user-F, denoted by $\mathcal{O}_{\mathrm{F}}$, is derived as follows.

$$\begin{aligned}\mathcal{O}_{\mathrm{F}} &= Pr(\Gamma_{\mathrm{N}}^{s_{\mathrm{F}}} < \gamma_{\mathrm{th}}, \Gamma_{\mathrm{F}}^{s_{\mathrm{F}}} < \gamma_{\mathrm{th}}) \\ &\quad + Pr(\Gamma_{\mathrm{N}}^{s_{\mathrm{F}}} > \gamma_{\mathrm{th}}, max(\Gamma_{\mathrm{F}}^{s_{\mathrm{F}}}, \Gamma_{\mathrm{NF}}) < \gamma_{\mathrm{th}}) \\ &= \underbrace{Pr(\Gamma_{\mathrm{N}}^{s_{\mathrm{F}}} < \gamma_{\mathrm{th}})}_{\Theta_{1A}(\gamma_{\mathrm{th}})} \underbrace{Pr(\Gamma_{\mathrm{F}}^{s_{\mathrm{F}}} < \gamma_{\mathrm{th}})}_{\Theta_{1B}(\gamma_{\mathrm{th}})} + \\ &\quad \underbrace{Pr(\Gamma_{\mathrm{F}}^{s_{\mathrm{F}}} < \gamma_{\mathrm{th}})}_{\Theta_{1B}(\gamma_{\mathrm{th}})} \underbrace{Pr(\Gamma_{\mathrm{N}}^{s_{\mathrm{F}}} > \gamma_{\mathrm{th}}, \Gamma_{\mathrm{NF}} < \gamma_{\mathrm{th}})}_{\Theta_{1C}(\gamma_{\mathrm{th}})}. \end{aligned} \tag{19}$$

In (19), in the first equality, $\gamma_{\mathrm{th}} = 2^{\frac{2R_{\mathrm{F}}}{1-\alpha}} - 1$, specifies the threshold for the SNR value to decode s_{F}, and R_{F} specifies user-F's data rate assuming that the events are independent of each other. The second equality is attained by considering the independent criteria between the users. After that, we will define each underbrace terms i.e., $\Theta_{1A}(\gamma_{\mathrm{th}})$, $\Theta_{1B}(\gamma_{\mathrm{th}})$, and $\Theta_{1C}(\gamma_{\mathrm{th}})$.

1) SOLUTION OF $\Theta_{1A}(\gamma_{\mathrm{TH}})$

Here, solving $\Theta_{1A}(\gamma_{th})$ by placing (8) in (19) and using the IQF canonical form produces

$$\Theta_{1A}(\gamma_{\mathrm{th}}) = Pr\left(\frac{(1-\rho)p_{\mathrm{F}}P_s||\tilde{\mathbf{h}}_{\mathrm{N}}||^2_{\mathbf{P}_{\mathrm{N}}}}{(1-\rho)p_{\mathrm{N}}P_s||\tilde{\mathbf{h}}_{\mathrm{N}}||^2_{\mathbf{P}_{\mathrm{N}}}+1} < \gamma_{\mathrm{th}}\right). \tag{20}$$

The following is the closed-form equation of (20) written as

$$\begin{aligned}\Theta_{1A}(\gamma_{\mathrm{th}}) &= 1 - \sum_{i=1}^{M} \frac{\lambda_{iN}}{\prod_{j=1,j\neq i}^{M}(\lambda_{iN}-\lambda_{jN})} \\ &\quad \times \exp\left(\frac{-\gamma_{\mathrm{th}}\left((1-\rho)\sigma_{\mathrm{N}}^2 \mathrm{tr}(\tilde{\mathbf{r}}_{\mathrm{N}}^H \mathbf{R}_{\mathrm{N}j-Rx})\right)}{\lambda_{iN}}\right) \\ &\quad \times \mathrm{u}\left(\frac{\gamma_{\mathrm{th}}\left((1-\rho)\sigma_{\mathrm{N}}^2 \mathrm{tr}(\tilde{\mathbf{r}}_{\mathrm{N}}^H \mathbf{R}_{\mathrm{N}j-Rx})\right)}{\lambda_{iN}}\right), \end{aligned} \tag{21}$$

where λ_{iN} is the ith eigenvalue of $\mathbf{P}_{\mathrm{N}}$ which is the function of γ_{th}.

Proof: *See Appendix A.*

Notably, in (21), $\mathbf{P}_{\mathrm{N}}$ regarded as:

$$\mathbf{P}_{\mathrm{N}} = \mathbf{A} - \mathbf{B}\gamma_{th}$$

where, $\mathbf{A}$ and $\mathbf{B}$ are Hermitian matrices, and γ_{th} represents a threshold parameter. Next, in (21) we perform the eigenvalue decomposition of $\mathbf{P}_{\mathrm{N}}$, denoted as:

$$\mathbf{P}_{\mathrm{N}} = U_p \Lambda_p U_p^H$$

where U_p is a unitary matrix composed of eigenvectors, and Λ_p is a diagonal matrix containing eigenvalues. This decomposition enables us to re-express (20) in a more analytically manageable form, offering insights into the structural properties of the matrices involved.

2) SOLUTION OF $\Theta_{1B}(\gamma_{\mathrm{TH}})$

Now, for the case of $\Theta_{1B}(\gamma_{\mathrm{th}})$, the conditional CDF of $\Theta_{1B}(\gamma_{\mathrm{th}})$ is expressed as

$$\Theta_{1B}(\gamma_{\mathrm{th}}) = Pr\left(\Gamma_{\mathrm{F}}^{s_{\mathrm{F}}} < \gamma_{\mathrm{th}}\right) \tag{22}$$

$$= Pr\left(\frac{||\tilde{\mathbf{h}}_{\mathrm{F}}||^2_{\mathbf{P}_{\mathrm{F}}}}{||\tilde{\mathbf{h}}_{\mathrm{F}}||^2_{\mathbf{P}_{\mathrm{F}}} + \sigma_{\mathrm{F}}^2 \mathrm{tr}(\tilde{\mathbf{r}}_{\mathrm{F}}^H \mathbf{r}_{\mathrm{F}})} < \gamma_{\mathrm{th}}\right). \tag{23}$$

The closed-form expression is written as follows:

$$\begin{aligned}\Theta_{1B}(\gamma_{\mathrm{th}}) &= 1 - \sum_{i=1}^{M} \frac{\lambda_{i\mathrm{F}}}{\prod_{j=1,j\neq i}^{M}(\lambda_{i\mathrm{F}}-\lambda_{j\mathrm{F}})} \\ &\quad \times \exp\left(\frac{-\gamma_{\mathrm{th}}\left((1-\rho)\sigma_{\mathrm{F}}^2 \mathrm{tr}(\tilde{\mathbf{r}}_{\mathrm{F}}^H \mathbf{r}_{\mathrm{F}})\right)}{\lambda_{i\mathrm{F}}}\right) \times \\ &\quad \times \mathrm{u}\left(\frac{\left((1-\rho)\sigma_{\mathrm{F}}^2 \mathrm{tr}(\tilde{\mathbf{r}}_{\mathrm{F}}^H \mathbf{r}_{\mathrm{F}})\right)}{\lambda_{i\mathrm{F}}}\right), \end{aligned} \tag{24}$$

where $\lambda_{i\mathrm{F}}$ is the ith eigenvalue of $\mathbf{P}_{\mathrm{F}}$, and the eigenvalues are the function of γ_{th}.

Proof: *In a similar way as in Appendix A.*

Notably, (21) and (24) play a crucial role in our analytical framework by providing insights into eigenvalue multiplicity and facilitating the transformation of matrices to a more analytically convenient form. This transformation enhances the interpretability and tractability of our results.

3) SOLUTION OF $\Theta_{1C}(\gamma_{\mathrm{TH}})$

Now, $\Theta_{1C}(\gamma_{\mathrm{th}})$ from (19) is

$$\Theta_{1C}(\gamma_{\mathrm{th}}) = Pr(\Gamma_{\mathrm{N}}^{s_{\mathrm{F}}} > \gamma_{\mathrm{th}}, \Gamma_{\mathrm{NF}} < \gamma_{\mathrm{th}}). \tag{25}$$

We deduce the closed-form expression as

$$\begin{aligned}&\Theta_{1C}(\gamma_{\mathrm{th}}) \\ &= \left[\exp\left(-\frac{\mu}{d_{\mathrm{N}}||\mathbf{P}_{\mathrm{N}}||^2}\right) - \frac{1}{d_{\mathrm{N}}}\Phi\left(\mu, \frac{1}{d_{\mathrm{N}}}, \frac{\gamma_{\mathrm{th}}}{d_{\mathrm{NF}}c}\right)\right], \end{aligned} \tag{26}$$

where $c = \frac{\eta P_s(2\alpha+(1-\alpha)\rho)}{(\sigma_{\mathrm{F}}^2+\sigma_{\mathrm{NF}}^2)(1-\alpha)}$.

Proof: *See Appendix B.*

Finally, the approximate expression of user-F's outage probability using a closed-form equation for distinct beamformers as given in (27), shown at the bottom of the next page.

B. OUTAGE PROBABILITY OF USER-N

By considering that the beamformers $\mathbf{w}_{\mathrm{N}}$ and $\mathbf{w}_{\mathrm{F}}$ are distinct, user-N's outage probability i.e., $\mathcal{O}_{\mathrm{N}}$, is written as

$$\mathcal{O}_{\mathrm{N}} = Pr\left(\Gamma_{\mathrm{N}}^{s_{\mathrm{N}}} < \gamma_{\mathrm{th}}\right). \tag{29}$$

In (29), the independent criterion between the users is applied.

Now using (9) in (29), we obtain

$$\mathcal{O}_{\mathrm{N}} = Pr\left(\frac{(1-\rho)p_{\mathrm{N}}P_s||\bar{\mathbf{h}}_{\mathrm{N}}||^2_{\mathbf{P}_{\mathrm{N}}}}{(1-\rho)\sigma^2_{\mathrm{N}}\mathrm{tr}(\tilde{\mathbf{r}}^H_{\mathrm{N}}\,\mathbf{R}_{\mathrm{N}j-Rx})} < \gamma_{\mathrm{th}}\right). \tag{30}$$

The exact closed-form expression of $\mathcal{O}_{\mathrm{N}}$ is written as (28), shown at the bottom of the page.

Proof: *The proof of (28) follows the IQF framework.*

IV. STATISTICAL BEAMFORMER DESIGN

In this section, different statistical beamforming schemes are proposed to minimize user-F's outage probability given in (27). For both outage probability and spectrum improvement, NOMA allows the sent messages to be superposed and forwarded in any time-frequency block. The transmitted messages are modulated to the BF vectors before transmission. In the presence of constraints that limit the transmit power, we define (27) as our objective function, which is optimized with respect to beamformer vectors. They can arrange the broadcast signals and use spatial dimensions to manage interference, allowing this SIC approach in NOMA to relay sensitive information to the intended users by using the same radio resources. To further improve the outage probability of user-F, we formulate the following multi-objective optimization problem.

$$\begin{aligned}
\mathbf{P}_1 : \underset{\mathbf{w}_{\mathrm{N}},\mathbf{w}_{\mathrm{F}},\mathbf{r}_{\mathrm{N}},\mathbf{r}_{\mathrm{F}},\mathbf{r}_{\mathrm{NF}}}{\text{minimize}}\ & \mathcal{O}_{\mathrm{F}}\left(\mathbf{w}_{\mathrm{N}},\mathbf{w}_{\mathrm{F}},\mathbf{r}_{\mathrm{N}},\mathbf{r}_{\mathrm{F}},\mathbf{r}_{\mathrm{NF}}\right)\\
\text{subject to} C1 : & ||\mathbf{w}_{\mathrm{N}}||^2 = ||\mathbf{w}_{\mathrm{F}}||^2 = 1\\
& ||\mathbf{r}_{\mathrm{N}}||^2 = ||\mathbf{r}_{\mathrm{F}}||^2 = ||\mathbf{r}_{\mathrm{NF}}||^2 = 1\\
& C2 : (\mathcal{O}_{\mathrm{N}})^{i+1} \le (\mathcal{O}_{\mathrm{N}})^{i}\\
& C3 : (\mathcal{O}_{\mathrm{F}})^{i+1} \le (\mathcal{O}_{\mathrm{F}})^{i},
\end{aligned} \tag{31}$$

where the number of iterations is indicated by the postscript i. The C1 constraint specifies that the norm of beamformers is equal to 1. We apply an exhaustive search to solve this non-convex and non-linear single objective constrained optimization problem as an exhaustive search assures finding the best solution from the domain selected. Algorithm I provides a pseudocode for the outage minimization task in (31).

We have used an exhaustive search method to solve this non-convex and non-linear single-objective constrained optimization problem. However, alternative methods like Successive Convex Approximation (SCA) and Random Matrix Theory (RMT) can be employed to enhance the scalability and efficiency of solving $\mathbf{P}_1$. We can discuss these two methods highlighting their potential benefits and limitations in the context of our specific optimization problem.

Successive Convex Approximation (SCA):

SCA involves converting a non-convex optimization problem into a convex one, which can be more efficiently solved using established convex optimization techniques. In the work by [33], a non-convex problem is transformed using series approximations and then solved in two stages. This method ensures faster convergence and can handle larger systems more effectively.

Pros:

- Efficient and faster convergence compared to exhaustive search.
- More scalable for larger systems.

Cons:

- The accuracy depends on the quality of the approximation.
- May converge to a local optimum rather than a global one.

Random Matrix Theory (RMT):

RMT simplifies the problem of supporting massive connectivity in NOMA systems. Bing et al. [34] demonstrate the use of RMT to design an autoconfigurable NOMA scheme, significantly improving user load and performance. This method is particularly suitable for scenarios involving a large number of devices.

Pros:

- Handles massive connectivity efficiently.
- Provides near-capacity performance and improved throughput.

$$\begin{aligned}
\mathcal{O}_{\mathrm{F}} = & \left[\left(1 - \sum_{i=1}^{M} \frac{\lambda_{i\mathrm{F}}}{\prod_{j=1,j\neq i}^{M}(\lambda_{i\mathrm{F}} - \lambda_{j\mathrm{F}})} \frac{\lambda_{i\mathrm{F}}}{\gamma_{\mathrm{th}}\lambda_{i\mathrm{F}} + \lambda_{jF}} \exp\left(\frac{-\gamma_{\mathrm{th}}\left(\sigma^2_{\mathrm{F}}(1-\rho)\mathrm{tr}(\tilde{\mathbf{r}}^H_F\,\mathbf{r}_F)\right)}{\lambda_{i\mathrm{F}}}\right)\right)\right]\\
& \times \left[\left(1 - \sum_{i=1}^{M} \frac{\lambda_{iN}}{\prod_{j=1,j\neq i}^{M}(\lambda_{iN} - \lambda_{jN})} \exp\left(\frac{-\gamma_{\mathrm{th}}\left((1-\rho)\sigma^2_{\mathrm{N}}\mathrm{tr}(\tilde{\mathbf{r}}^H_{\mathrm{N}}\,\mathbf{R}_{\mathrm{N}j-Rx})\right)}{\lambda_{iN}}\right) \mathrm{u}\left(\frac{\gamma_{\mathrm{th}}\left((1-\rho)\sigma^2_{\mathrm{N}}\mathrm{tr}(\tilde{\mathbf{r}}^H_{\mathrm{N}}\,\mathbf{R}_{\mathrm{N}j-Rx})\right)}{\lambda_{iN}}\right)\right)\right.\\
& \left. + \left[\exp\left(-\frac{\mu}{d_{\mathrm{N}}||\mathbf{P}_{\mathrm{N}}||^2}\right) - \frac{1}{d_{\mathrm{N}}}\Phi\left(\mu, \frac{1}{d_{\mathrm{N}}}, \frac{\gamma_{\mathrm{th}}}{d_{\mathrm{NF}}c}\right)\right]\right].
\end{aligned} \tag{27}$$

$$\mathcal{O}_{\mathrm{N}} = \left[\left(1 - \sum_{i=1}^{M} \frac{\lambda_{i\mathrm{N}}}{\prod_{j=1,j\neq i}^{M}(\lambda_{i\mathrm{N}} - \lambda_{j\mathrm{N}})} \frac{\lambda_{i\mathrm{N}}}{\gamma_{\mathrm{th}}\lambda_{i\mathrm{N}} + \lambda_{j\mathrm{N}}} \exp\left(\frac{-\gamma_{\mathrm{th}}\left(\sigma^2_{\mathrm{N}}(1-\rho)\mathrm{tr}(\tilde{\mathbf{r}}^H_{\mathrm{N}}\,\mathbf{R}_{\mathrm{N}j-Rx})\right)}{\lambda_{i\mathrm{N}}}\right)\right)\right] \tag{28}$$

TABLE 3. Outage minimization task.

Input: Initialized beamformers $\mathbf{w}_N$, $\mathbf{w}_F$, $\mathbf{r}_N$, $\mathbf{r}_F$, and $\mathbf{r}_{NF}$
Output: Optimized beamformers $\mathbf{w}_N$, $\mathbf{w}_F$, $\mathbf{r}_N$, $\mathbf{r}_F$, and $\mathbf{r}_{NF}$
1. Initialize $\mathbf{w}_N$, $\mathbf{w}_F$, $\mathbf{r}_N$, $\mathbf{r}_F$, and $\mathbf{r}_{NF}$ set threshold level (ζ), precision , number of iteration (i)
2. Repeat
3. Compute $\mathcal{O}_F$ as in (31)
4. $i = i + 1$
5. Compute $(\mathcal{O}_F)^{i+1}$, $(\mathcal{O}_N)^{i+1}$ as in (31)
6. If $\{(\mathcal{O}_N)^{i+1} \leq (\mathcal{O}_N)^i\}$
7. Store beamformer value, $\mathcal{O}_N$, then perform recursion
8. Else
9. Return optimized beamformer value, $\mathcal{O}_N$,
10. Stop Condition = True
11. End if
12. Until (Condition = True)

Cons:

- Mathematically intensive and complex to implement.
- Applicability may be limited to specific network types.

So, if we evaluate the applicability given the nature of our optimization problem $\mathbf{P}_1$, SCA presents a promising alternative due to its ability to transform and solve non-convex problems efficiently. However, the potential for approximation errors and local optima needs careful consideration. RMT offers significant advantages for large-scale systems, but its complexity and specific applicability warrant further investigation.

A. RECEIVE BEAMFORMING DESIGN FOR COVARIANCE SHAPING

The BS will spatially isolate the signals corresponding to various users in a MIMO-NOMA network on the bases of different power levels assigned to each user and whether their covariance matrices are on orthogonal, i.e., $\Sigma_N \Sigma_F = 0$. In this context, we develop a UE-side covariance shaping solution that is solely focused on channel statistical knowledge, with the intention of implementing the aforementioned channel statistics orthogonality. Correspondingly, the sub-optimal and low complex solutions for receive beamforming vectors $\mathbf{r}_N$, $\mathbf{r}_F$, and $\mathbf{r}_{NF}$ in case of direct and relaying transmissions are presented as follows.

1) DIRECT TRANSMISSION CASE

In case of from the BS to user-N, the objective function for the receive beamformer $\mathbf{r}_N$ is set to be the product of the matrices of effective covariance. The aim herein is to achieve orthogonality among the cross-covariance of the users and is given as

$$\Upsilon(\mathbf{r}_N, \mathbf{r}_F, \mathbf{r}_{NF}) = \underset{||\mathbf{r}_N||^2=||\mathbf{r}_F||^2=||\mathbf{r}_{NF}||^2=1}{\arg\min} \Psi_N \Psi_F \Psi_{NF}. \quad (32)$$

Here Ψ_N, Ψ_F, and Ψ_{NF} represent the corresponding channel covariance matrices.

However, a closed-form solution for (32) is not available. For our case of a two-users cooperative MIMO-NOMA system, a sub-optimal, low complex solution to problem in (32), can be obtained, for instance, via alternate optimization given as

$$\mathbf{P}_2(\mathbf{a}): \quad \min_{\mathbf{r}_N} \frac{\mathbf{r}_N^H \sum_{x,y=1}^{M} \left(\left(\frac{\mathbf{r}_F^H \Sigma_F^{x,y} \mathbf{r}_F}{\mathbf{r}_F^H \mathbf{R}_F \mathbf{r}_F} \right) \Sigma_N^{x,y} + \left(\frac{\mathbf{r}_{NF}^H \Sigma_{NF}^{x,y} \mathbf{r}_{NF}}{\mathbf{r}_{NF}^H \mathbf{R}_{NF} \mathbf{r}_{NF}} \right) \Sigma_{NF}^{x,y} \right) \mathbf{r}_N}{\mathbf{r}_N^H \mathbf{R}_N \mathbf{r}_N}$$

$$\text{subject to} \quad || \mathbf{R}_{Nj-Rx} ||^2 = 1. \quad (33)$$

Using the minimum eigenvector of

$$\mathbf{R}_N^{-1} \sum_{x,y=1}^{M} \left(\left(\frac{\mathbf{r}_F^H \Sigma_F^{x,y} \mathbf{r}_F}{\mathbf{r}_F^H \mathbf{R}_F \mathbf{r}_F} \right) \Sigma_N^{x,y} + \left(\frac{\mathbf{r}_{NF}^H \Sigma_{NF}^{x,y} \mathbf{r}_{NF}}{\mathbf{r}_{NF}^H \mathbf{R}_{NF} \mathbf{r}_{NF}} \right) \Sigma_{NF}^{x,y} \right)$$

when the objective is in the G-RQ form, we obtain the solution.

Similarly, in the case of from the BS to user-F, the objective function for the receive beamformer $\mathbf{r}_F$, is the same as expressed in (32) and a sub-optimal, low complex solution via alternate optimization is given as

$$\mathbf{P}_2(\mathbf{b}): \quad \min_{\mathbf{r}_F} \frac{\mathbf{r}_F^H \sum_{x,y=1}^{M} \left(\left(\frac{\mathbf{r}_N^H \Sigma_N^{x,y} \mathbf{r}_N}{\mathbf{r}_N^H \mathbf{R}_N \mathbf{r}_N} \right) \Sigma_F^{x,y} + \left(\frac{\mathbf{r}_{NF}^H \Sigma_{NF}^{x,y} \mathbf{r}_{NF}}{\mathbf{r}_{NF}^H \mathbf{R}_{NF} \mathbf{r}_{NF}} \right) \Sigma_{NF}^{x,y} \right) \mathbf{r}_F}{\mathbf{r}_F^H \mathbf{R}_F \mathbf{r}_F}$$

$$\text{subject to} \quad ||\mathbf{r}_F||^2 = 1. \quad (34)$$

In this case, the minimum eigenvector provides the solution of

$$\mathbf{R}_F^{-1} \sum_{x,y=1}^{M} \left(\left(\frac{\mathbf{r}_N^H \Sigma_N^{x,y} \mathbf{r}_N}{\mathbf{r}_N^H \mathbf{R}_N \mathbf{r}_N} \right) \Sigma_F^{x,y} + \left(\frac{\mathbf{r}_{NF}^H \Sigma_{NF}^{x,y} \mathbf{r}_{NF}}{\mathbf{r}_{NF}^H \mathbf{R}_{NF} \mathbf{r}_{NF}} \right) \Sigma_{NF}^{x,y} \right)$$

when the objective is in the G-RQ form.

The values of $\mathbf{r}_N$ and $\mathbf{r}_F$ are found by alternating minimization until the gap between the objectives in successive iterations is small enough. It is worth noting that each user can obtain a covariance shaping vector as its own without exchanging any information with other users.

2) RELAYING TRANSMISSION CASE

For the relaying transmission case, we assume that beamforming is performed by the BS as it has sufficient capacity to handle the computationally complex task (e.g., optimization) better than user-N. The objective function for the receive beamformer $\mathbf{r}_{NF}$ is written the same way as in (32), whereas, a sub-optimal, low complex solution to the problem formulated in (32) is achieved via alternate optimization expressed as

$$\mathbf{P}_2(\mathbf{c}): \quad \min_{\mathbf{r}_{NF}} \frac{\mathbf{r}_{NF}^H \sum_{x,y=1}^{M} \left(\left(\frac{\mathbf{r}_N^H \Sigma_N^{x,y} \mathbf{r}_N}{\mathbf{r}_N^H \mathbf{R}_N \mathbf{r}_N} \right) \Sigma_F^{x,y} + \left(\frac{\mathbf{r}_F^H \Sigma_{F,mn} \mathbf{r}_F}{\mathbf{r}_F^H \mathbf{R}_F \mathbf{r}_F} \right) \Sigma_{F,mn} \right) \mathbf{r}_{NF}}{\mathbf{r}_{NF}^H \mathbf{R}_{NF} \mathbf{r}_{NF}}$$

$$\text{subject to} \quad ||\mathbf{r}_{NF}||^2 = 1. \quad (35)$$

TABLE 4. Covariance shaping.

Input: Σ_{N}, Σ_{F}, Σ_{NF}, $\mathbf{r}_{\mathrm{N}}$, $\mathbf{r}_{\mathrm{F}}$, and $\mathbf{r}_{\mathrm{NF}}$
Output: Optimized receive beamformers $\mathbf{r}_{\mathrm{N}}$, $\mathbf{r}_{\mathrm{F}}$, and $\mathbf{r}_{\mathrm{NF}}$
1. Initialize $\mathbf{r}_{\mathrm{N}}$, $\mathbf{r}_{\mathrm{F}}$, and $\mathbf{r}_{\mathrm{NF}}$, threshold (ζ),
precison, time index (i), and number of iterations.
2. Repeat
3. while $|\Upsilon(\mathbf{r}_{\mathrm{N}}^{i}, \mathbf{r}_{\mathrm{F}}^{i}, \mathbf{r}_{\mathrm{NF}}^{i}) - \Upsilon(\mathbf{r}_{\mathrm{N}}^{i-1}, \mathbf{r}_{\mathrm{F}}^{i-1}, \mathbf{r}_{\mathrm{NF}}^{i-1}|/\Upsilon(\mathbf{r}_{\mathrm{N}}^{i}, \mathbf{r}_{\mathrm{F}}^{i}, \mathbf{r}_{\mathrm{NF}}^{i}) > \zeta$
4. Compute $\mathbf{r}_{\mathrm{N}}^{i}, \mathbf{r}_{\mathrm{F}}^{i}, \mathbf{r}_{\mathrm{NF}}^{i}$ as in (33), (34), and (35) respectively
5. $i = i + 1$
4. Compute $\mathbf{r}_{\mathrm{N}}^{i+1}, \mathbf{r}_{\mathrm{F}}^{i+1}, \mathbf{r}_{\mathrm{NF}}^{i+1}$
6. If $\{(\mathbf{r}_{\mathrm{N}})^{i+1} \leq (\mathbf{r}_{\mathrm{N}})^{i}\}, \{(\mathbf{r}_{\mathrm{F}})^{i+1} \leq (\mathbf{r}_{\mathrm{F}})^{i}\}, \{(\mathbf{r}_{\mathrm{NF}})^{i+1} \leq (\mathbf{r}_{\mathrm{NF}})^{i}\}$
7. Store receive beamformer values, then perform recursion
8. Else
9. Return optimized receive beamformer value
10. Stop Condition = True
11. End if
12. End while
13. Until (Condition = True)

Again, the minimum eigenvector solution of (35) is obtained as

$$\mathbf{R}_{\mathrm{NF}}^{-1} \sum_{x,y=1}^{M} \left(\left(\frac{\mathbf{r}_{\mathrm{N}}^{H} \Sigma_{\mathrm{N}}^{x,y} \mathbf{r}_{\mathrm{N}}}{\mathbf{r}_{\mathrm{N}}^{H} \mathbf{R}_{\mathrm{N}} \mathbf{r}_{\mathrm{N}}} \right) \Sigma_{\mathrm{F}}^{x,y} + \left(\frac{\mathbf{r}_{\mathrm{F}}^{H} \Sigma_{\mathrm{F},mn} \mathbf{r}_{\mathrm{F}}}{\mathbf{r}_{\mathrm{F}}^{H} \mathbf{R}_{\mathrm{F}} \mathbf{r}_{\mathrm{F}}} \right) \Sigma_{\mathrm{F},mn} \right)$$

when the objective is in the G-RQ form. The pseudo-code for the covariance shaping is given in Algorithm II.

B. TRANSMIT BEAMFORMING DESIGN FOR MINIMIZATION OF OUTAGE PROBABILITY OF USER-F BASED ON G-RQ

Using an SINR-based optimization criterion, the transmit beamformer could be designed to optimize a related metric such as the sum rate. However, as each user's SINR is nonconvexly dependent on transmit beamformers, this requirement usually leads to a difficult nonconvex optimization problem. To resolve this issue, we adopt the signal-to-leakage-plus-noise ratio (SLNR) solution. In the SLNR solution, instead of including the total interference power obtained at the specific receiver, we have included the power of total interference plus noise. The rationale for this approach is that, in multi-user interference networks, it is fair for a transmitter to optimize the power of the signal to its receiver.

To improve the outage probability of user-F, during both direct and relaying transmissions, transmit beamforming is designed as

$$f(\mathbf{w}_{\mathrm{N}}, \mathbf{w}_{\mathrm{F}}) = \underset{||\mathbf{w}_{\mathrm{N}}||^2 = ||\mathbf{w}_{\mathrm{F}}||^2 = 1,}{\arg\min} \quad \mathcal{O}_{\mathrm{F}}(\mathbf{w}_{\mathrm{N}}, \mathbf{w}_{\mathrm{F}}, \mathbf{r}_{\mathrm{N}}, \mathbf{r}_{\mathrm{F}}, \gamma_{\mathrm{th}}). \tag{36}$$

We develop a sub-optimal solution based on transmitting SLNR statistics instead of the SINR as the metric because an improvement in SLNR correlates to a rise in SINR and vice versa. Furthermore, our solution is undefined because it implies channel covariance information instead of instantaneous CSI. As a result, the problem of G-RQ maximization is formulated as

$$\mathbf{P}_3: \quad \underset{\mathbf{w}_{\mathrm{F}}}{\text{maximize}} \frac{\mathbf{w}_{\mathrm{F}}^{H} \left(\mathbb{E}\left[\mathbf{h}_{\mathrm{F}}^{H} \mathbf{h}_{\mathrm{F}} \right] \right) \mathbf{w}_{\mathrm{F}}}{\mathbf{w}_{\mathrm{N}}^{H} \left(\mathbb{E}\left[\mathbf{h}_{\mathrm{N}}^{H} \mathbf{h}_{\mathrm{N}} \right] + \sigma_{\mathrm{F}}^{2} \mathbf{I}_{\mathrm{N}} \right) \mathbf{w}_{\mathrm{N}}}$$
$$\text{subject to} \quad ||\mathbf{w}_{\mathrm{N}}||^2 = ||\mathbf{w}_{\mathrm{F}}||^2 = 1. \tag{37}$$

The solution to the above-mentioned maximization problem is the eigenvector, which is related to the eigenvalue of $\left[\Psi_{\mathrm{N}} + \sigma_{\mathrm{F}}^{2} \mathbf{I}_{\mathrm{N}}\right]^{-1} \Psi_{\mathrm{F}}$.

V. ITERTIVE RESOURCE ALLOCATION SCHEME

This section introduces the proposed power allocation and power splitting algorithms for the SWIPT MIMO-NOMA systems. The first stage is to separate problem P1 into two subproblems: one to determine the ideal PS ratio with fixed values of power allocation, and another to investigate the best power allocation with a fixed PS ratio. Furthermore, both the equal and independent PS ratio cases are taken into account to achieve better results.

A. POWER SPLITTING CONTROL WITH FIXED POWER ALLOCATION CASE

We define the subproblem of optimization to find the best PS ratio with a fixed power allocation coefficient and propose an efficient algorithm for determining the PS ratio for both users.

The mathematical formulation of the associated subproblem with fixed power allocation is as follows:

$$\mathbf{P}_4: \quad \underset{\rho}{\text{minimize}} \mathcal{O}_{\mathrm{F}}(\rho)$$
$$\text{subject to} \quad C1: (\mathcal{O}_{\mathrm{N}})^{i+1} \leq (\mathcal{O}_{\mathrm{N}})^{i}$$
$$C2: 0 < \rho < 1. \tag{38}$$

Here, for the case of $\rho = 0$, the signals received from the BS by user-N are solely used to decode the information, and user-N cannot harvest any energy. Therefore, the power splitting factor should be in the range of $0 < \rho < 1$. Furthermore, for NOMA with fixed power allocation (F-NOMA), the power allocation coefficients (PACs) for both user-N and user-F are constants. The PACs are not functions of the users' channel gains in this case. In this situation, the transmitter just needs to know the order of channel gains among users in order to facilitate NOMA.

It is noted that to collect source energy at user-N, the power splitting protocol is employed and this power splitting for energy harvesting is over time. In addition, the decode-and-forward protocol is used by user-N to decode the information from the BS. Because of these considerations, user-N must first confirm that the messages from the BS are identified before moving on to energy harvesting. We suppose that user-N can successfully decode both s_{F} and s_{N} signals. Then the power splitting factor ρ is provided based on this

TABLE 5. Optimization of PACs and PS factor.

Input: Initialized power splitting ratio ρ
Output: Optimized ρ value
1. Randomly initialize PS ratio ρ, $0 < \rho < 1$, threshold (ζ), precison, time index (i), and iteration numbers
2. Solve problem **P5** using (40) and (42), record power allocation coefficients p_{N} and p_{F}
3. **REPEAT**
4. Solve problem **P4** using (39) and record the PS ratio ρ
5. If $\mathcal{O}_{\mathrm{F}}(\rho)^{(i)} - \mathcal{O}_{\mathrm{F}}(p_{\mathrm{N}}, p_{\mathrm{F}})^{(i-1)} > \zeta$
6. Solve problem **P5** using (40) and (42), record power allocation coefficients p_{N} and p_{F}
7. If $\mathcal{O}_{\mathrm{F}}(p_{\mathrm{N}}, p_{\mathrm{F}})^{(i)} - \mathcal{O}_{\mathrm{F}}(\rho)^{(i)} < \zeta$
8. Return $p_{\mathrm{N}}^{\mathrm{opt}} = p_{\mathrm{N}}^{i-1}$, $\rho^{\mathrm{opt}} = \rho^{i}$
9. End
10. Else
11. Return $p_{\mathrm{N}}^{\mathrm{opt}} = p_{\mathrm{N}}^{i-1}$, $\rho^{opt} = \rho^{i-1}$
12. Condition = True,
13. End
14. **Until** (Condition = True)

assumption as.

$$\rho = \max\left\{0, 1 - \frac{2^{2R_{\mathrm{th,N}}+2R_{\mathrm{th,F}}} - 1}{P_s ||\mathbf{h}_{\mathrm{N}}||^2_{\mathbf{P}_{\mathrm{N}}}}\right\}, \tag{39}$$

where $R_{\mathrm{th,N}}$ and $R_{\mathrm{th,F}}$ (bits/s/Hz) are the spectral efficiencies to decode s_{N} and s_{F}, respectively, and can be obtained as

$$\begin{cases} R_{\mathrm{th,N}} = & \frac{1}{2} log_2\left(1 + \frac{p_{\mathrm{N}} P_s ||\bar{\mathbf{h}}_{\mathrm{N}}||^2_{\mathbf{P}_{\mathrm{N}}}}{\sigma^2_{\mathrm{N}} \mathrm{tr}(\tilde{\mathbf{r}}^H_{\mathrm{N}} \mathbf{R}_{\mathrm{N}j-Rx})}\right) \\ R_{\mathrm{th,F}} = & \frac{1}{2} log_2\left(\frac{|\mathbf{R}_{\mathrm{N}j-Rx} \mathbf{H}_{\mathrm{N}} \mathbf{w}_{\mathrm{B}}|^2 p_{\mathrm{F}} P_s}{|\mathbf{R}_{\mathrm{N}j-Rx} \mathbf{H}_{\mathrm{N}} \mathbf{w}_{\mathrm{B}}|^2 p_{\mathrm{N}} P_s + |\mathbf{R}_{\mathrm{N}j-Rx} \mathbf{v}_{\mathrm{N}}|^2}\right). \end{cases} \tag{40}$$

B. POWER ALLOCATION CONTROL WITH FIXED POWER SPLITTING CASE

The corresponding subproblem of finding the best power allocation coefficient with fixed PS ratios is expressed mathematically as

$$\begin{aligned} \mathbf{P}_5: \quad & \underset{p_{\mathrm{N}}, p_{\mathrm{F}}}{\text{minimize}} \mathcal{O}_{\mathrm{F}}(p_{\mathrm{N}}, p_{\mathrm{F}}) \\ \text{subject to} \quad & C1: (\mathcal{O}_{\mathrm{N}})^{i+1} \leq (\mathcal{O}_{\mathrm{N}})^{i} \\ & C2: 0 < p_{\mathrm{N}} < p_{\mathrm{F}} \\ & C3: p_{\mathrm{N}} + p_{\mathrm{F}} = 1. \end{aligned} \tag{41}$$

With given PS ratios and transmit power, the objective function related to problem $\mathbf{P}_5$ is a concave function with respect to p_{N}, p_{F}, if $p_{\mathrm{N}}|h_{\mathrm{N}}|^2 < p_{\mathrm{F}}|h_{\mathrm{F}}|^2$. To solve $\mathbf{P}_5$, the PACs are determined before the energy harvesting process and it evaluates user-N's quality of service (QoS). The reason to choose user-N is that user-N involves decoding x_{N} and x_{F}, and SIC is also performed on this user. Furthermore, in this study a hybrid TS/PS framework is considered. Therefore, it is difficult to determine the PACs (p_{N}, p_{F}) independently. For example, in the expression of $2^{\frac{2R_{\mathrm{th,F}}}{1-\alpha}}$, the term α cannot be eliminated. Hence, the PACs of user-N and user-F are determined as

$$\begin{cases} p_{\mathrm{N}} = & \frac{2^{2R_{\mathrm{th,N}}} - 1}{2^{2R_{\mathrm{th,N}}+2R_{\mathrm{th,F}}} - 1} \\ p_{\mathrm{F}} = & 1 - p_{\mathrm{N}}. \end{cases} \tag{42}$$

The pseudo-code for the optimization of PACs and PS factor is given in Algorithm III.

TABLE 6. Simulation parameters [30], [32].

Parameters	Values
Bandwidth	1 MHz
Correlation coefficient χ_1	$0.2 + 0.4i$
Correlation coefficient χ_2	$0.1 + 0.3i$
Data rates of users, $R_{\mathrm{th,N}} = R_{\mathrm{th,F}}$	0.17 bits/s/Hz
Information decoding efficiency, η	0.7
Antenna noise power density, n_a	-100 dBm/Hz
Noise power density for information process, n_c	-90 dBm/Hz
The number of Monte-Carlo simulations	10^6
Path loss exponent, ϵ	3
BS and user-N distance, d_{N}	3 m
BS to user-F distance, d_{F}	10 m
user-N to user-F distance, d_{NF}	$d_{\mathrm{N}} - d_{\mathrm{F}}$

VI. NUMERICAL RESULTS AND DISCUSSIONS

This section contains results obtained based on the cooperative MIMO-NOMA network with Rayleigh fading channels. To validate the closed-form expressions derived in our study, we conducted Monte Carlo simulations using MATLAB R2016a. The simulations were executed on a computing platform equipped with an Intel® Core™ i7-7500U CPU @ 2.90 GHz 2.70 GHz and 16GB RAM.

A. CONFIGURATION OF PARAMETERS

The BS, user-N, and user-F are all considered to be on a straight line. In cooperative NOMA networks, this assumption has been broadly accepted, e.g., in [31]. This assumption is made in order to examine the impact of user-N's location on the performance of two-hop cooperative NOMA systems in which user-N moves along the horizon between BS and user-F. The distinct transmit and receive correlation matrices are given as $\mathbf{R}^{\frac{1}{2}}_{ij-Tx} = \chi_1^{|i-j|}$ and $\mathbf{R}^{\frac{1}{2}}_{ij-Rx} = \chi_2^{|i-j|}$, respectively, where the coefficients for correlation i.e., $\chi 1$ and $\chi 2$ are constrained from 0 to 1. In case of both the Kronecker structured and covariance shaping, we validate the formulas in (27) and (28). The beamformers for the general model with covariance shaping provided in (33), (34), (35), and (37), whereas the Kronecker structured model's beamformers take G-MRT into account. Unless stated otherwise, Table 6 lists the simulation parameters configured, which are widely used in other NOMA studies. These configurations are largely adapted from [30] and [32].

In our simulation setup, we model a line network configuration where user-N is located directly between the Base Station (BS) and user-F. This arrangement is a well-established assumption in both conventional cooperative

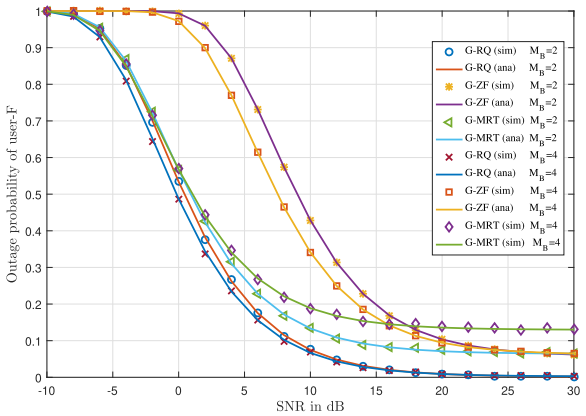

FIGURE 2. Comparison of G-RQ, G-MRT, and G-ZF channel models for $M_F = M_N = K = 2$.

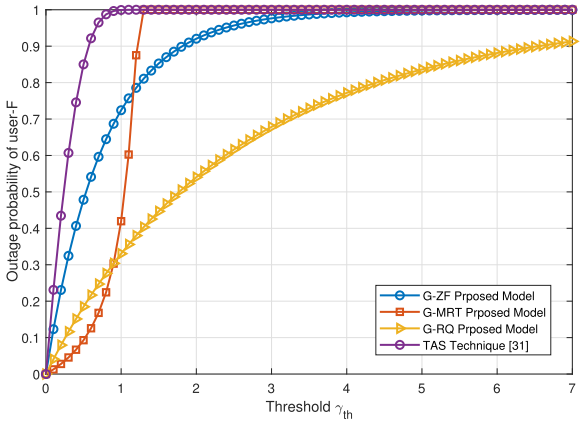

FIGURE 3. Comparison of the proposed model G-RQ, G-MRT, and G-ZF channel models with TAS technique for $M_B = 2, M_F = M_N = 4, K = 2$.

networks [35], [36] and cooperative NOMA networks, enlightened in [31] and [37]. The primary rationale for this setup is to facilitate the analysis of the impact of user-N's position on the performance of two-hop cooperative NOMA systems. Specifically, this configuration allows us to study scenarios where user-N moves along the direct line from the source (S) to user-F. Furthermore, we assume a path loss exponent of 3 for all wireless channels. This assumption is consistent with the values commonly adopted in prior research, as indicated in [38], [39], and [40]. It is worth noting that the path loss exponent for urban microcells typically ranges from 2.7 to 3.5, as highlighted in [41]. Therefore, selecting a path loss exponent of 3 is a realistic and widely accepted parameter for simulating signal attenuation in urban micro-cell environments. Furthermore, we have assumed 1MHz of bandwidth in our simulation setup as in [32], as it supports relaying to obtain further improvement on the coverage range [42].

B. OUTAGE PROBABILITY ANALYSIS OF USER-F

With an increase in SNR (in dB), the outage probability of user-F improves as shown in Fig. 2. It can be observed

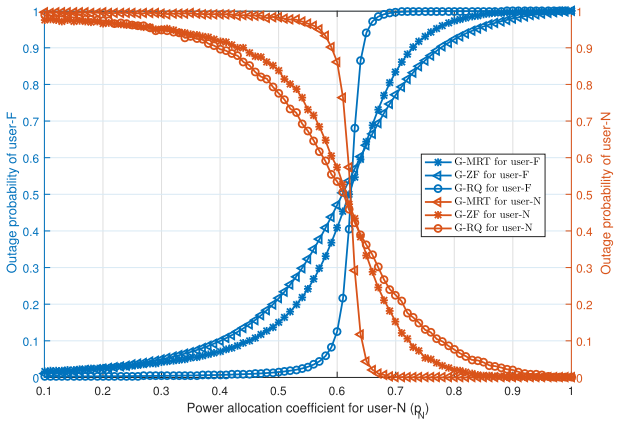

FIGURE 4. Impact of power allocation coefficient p_N on the outage probability of user-N and user-F for $M_B = 4, M_F = M_N = 2$.

that the covariance shaping-based channel model, i.e., G-RQ based on the transmit SLNR, has higher performance as compared to the G-MRT and G-ZF which are two reference statistical approaches. Because G-RQ mitigates leakage interference (which results in the elimination of co-channel interference (CCI)) and noise at the same time, it improves performance. G-MRT and G-ZF, on the other hand, only seek to increase SNR or reduce CCI. Across the SNR range, the simulation results match precisely the closed-form formulation. Furthermore, the impact of the transmit antenna and receive antenna can also be observed in Fig. 2.

In Fig. 1, a comparison between the proposed scheme and the transmit antenna selection (TAS) scheme in [32] is shown in a comparable arrangement. When compared to [32], the outage probability of user-F of the proposed scheme which employs using the SWIPT protocol indicates a better outage probability. In the case of the G-MRT, G-ZF, and G-RQ schemes, the comparison is displayed in the same figure. It is observed that at lower values of γ_{th} the performance of other statistical methods, i.e., G-MRT and G-ZF has better results while the transmit SLNR-based G-RQ schemes achieve better results when the values of the predefined threshold γ_{th} is increased. At $\gamma_{th} = 1$, the outage probability of user-F is 32%, 41%, 75%, and 99% for G-RQ, G-MRT, G-ZF, and TAS schemes, respectively, showing that our scheme outperforms the TAS scheme. Moreover, the outage probability of user-F increases across the γ_{th} values.

C. IMPACT OF POWER ALLOCATION COEFFICIENTS AND USER-N DISTANCE ON OUTAGE PROBABILITY OF USER-F

The impact of coefficients of power allocations of user-N on the outage probability of both users is shown in Fig. 4. The outage probability of user-F degrades when the value of p_N is increased. This is in accordance with the principle of NOMA, since, $p_N + p_F = 1$. The optimal value of the power allocation coefficient, i.e., $p_N = 0.62$ is achieved and the tradeoff between the outage probabilities of user-N and user-F can be noticed in Fig. 4. As a result, increasing the

TABLE 7. Comparison with recent works.

References	Transmit Scheme	Precoding vector	Performance metric	Optimization problem	Equalizing Vector
[46]	two-user-NOMA	×	Outage Probability	Fairness	×
[47]	two-user-NOMA	×	Sumrate	Optimized Power	×
[32]	two-user-NOMA	Orthonormal	Outage Probability	Transmit antenna selection	×
[48]	two-user MISO-NOMA	linear precoding	Sumrate	improper Gaussian signaling	×
[49]	two-user MIMO-NOMA	Orthonormal	Sumrate	Power allocation and Gain	Deterministic
[26]	two-user MIMO-NOMA	Optimized Vector	Outage Probability	Power Gain	Channel Equalization
Our work	two-user MIMO-NOMA system	Optimized vectors	Outage Probability	Iterative resource allocation	Covariance shaping

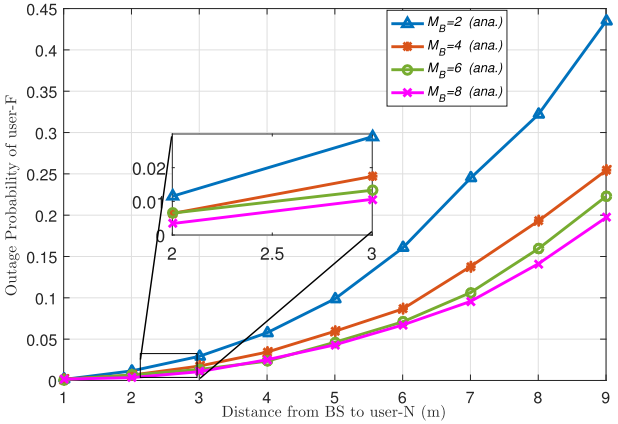

FIGURE 5. Outage probability of user-F as a function of distance of user-N from BS for G-RQ case for $M_N = M_F = 4$.

value of p_N lowers the p_F value, resulting in the degradation of user-F's outage probability, and vice versa.

To further evaluate the performance of user-F, we reconfigure the distance between user-N and user-F by assuming that the movement of user-N is away from the BS towards user-F in a straight line, as shown in Fig. 5. The outage probability rises when user-N is farther away from the BS. Furthermore, more the number of BS antennas, the lower the outage probability. As the distance between BS and user-N decreases, better outage probability performance of user-F is achieved. When user-N is farther away from the BS, the harvested energy value decreases, leading to less power for user-N to support user-F for relaying. Because of the SIC receiver at user-N, the non-identical channel conditions of users is significant in the NOMA system.

VII. COMPARISON

We derive the probability of outage in closed form for a multiuser multi-path MIMO system with a precoder and equalizer. Unlike previous approaches [43], [44], [45], which require Channel State Information (CSI), our work relies solely on the knowledge of transmit and receive correlation matrices. We have developed a comparison in Table 7 to highlight the significance of our proposed work in relation to recent studies [26], [32], [46], [47], [48], [49]. The comparison is based on key criteria, including Transmit Scheme, Precoding Vector, Performance Metric, Optimization Problem, and Equalizing Vector.

In our proposed work, we address both near-user (user-N) and far-user (user-F) scenarios in a two-user MIMO-NOMA system. This distinction is highlighted in Table 7, which showcases key differences from recent works on the indefinite quadratic forms approach. We also introduce iterative precoding and equalization techniques aimed at minimizing the outage probability derived in closed form. This approach differs significantly from the methods in [50], [51], and [52], which are based on the Minimum Mean Square Error (MMSE) criterion.

Overall, our work offers a novel perspective by designing precoder and equalizer strategies to minimize the probability of outage, thereby enhancing system performance and reliability.

VIII. CONCLUSION

In this paper, we have developed a transmit-relay-receive scheme for downlink data transmissions in a two-user MIMO-NOMA network, enabled by beamforming and SWIPT. Based on the deduced outage probability for both users in a Rayleigh fading channel condition, we formulate a multi-objective optimization problem considering transmit correlation, power allocation, and power splitting factors. Accordingly, we optimize the transmit and receive beams using an SLNR and covariance shaping based on the G-RQ technique. Through analytical and simulation results, we demonstrate that the proposed transmission and reception beamforming scheme based on G-RQ outperforms other reference schemes. Furthermore, our scheme can increase overall spectral efficiency as it is a undefined technique assuming only statistical CSI at the BS. Moreover, iterative algorithms are provided to optimize power allocation and power splitting factors. Finally, analytical results are validated through extensive simulations.

APPENDIX A

Proof of (21):

Utilizing the expression $\mathrm{u}(x) = \frac{1}{2\pi}\int_{-\infty}^{\infty}\frac{\exp((x)(iw+\beta))}{(iw+\beta)}dw$; $\beta > 0$ as in [30], we obtain

$$\Theta_{1A}(\mathrm{th}) = \frac{1}{2\pi^{N+1}}\int_{-\infty}^{\infty}\frac{\exp\left(\gamma_{\mathrm{th}}((1-\rho)\sigma_{a\mathrm{N}}^2+\sigma_{c\mathrm{N}}^2)(iw+\beta)\right)}{iw+\beta} \times \int_{-\infty}^{\infty}\exp\left(-||\bar{\mathbf{h}}_{\mathrm{N}}||^2_{\mathbf{I}+\mathbf{P}(iw+\beta)}\right)d\bar{\mathbf{h}}_{\mathrm{N}}dw. \quad (43)$$

Next, the unitary Hermitian matrix $\mathbf{P}$ after eigenvalue decomposition is performed, i.e., $\mathbf{P} = \mathbf{U}_p \wedge \mathbf{U}_p^{\mathbf{H}}$. The weight matrix which is of the diagonal form is obtained as a result of this transformation. As a result, we get

$$\begin{aligned}\Theta_{1A}(\text{th}) =& \frac{1}{2\pi^{N+1}} \int_{-\infty}^{\infty} \frac{\exp\left((\gamma_{\text{th}}((1-\rho)\sigma_{a\text{N}}^2 + \sigma_{c\text{N}}^2)(iw+\beta)\right)}{iw+\beta} \\ &\times \int_{-\infty}^{\infty} \exp\left(-||\tilde{\mathbf{h}}_{\text{N}}||^2_{\mathbf{I}+\wedge(iw+\beta)}\right) d\tilde{\mathbf{h}}_{\text{N}} dw \\ =& \frac{1}{2\pi} \int_{-\infty}^{\infty} \frac{\exp\left(\gamma_{\text{th}}((1-\rho)\sigma_{a\text{N}}^2 + \sigma_{c\text{N}}^2)(iw+\beta)\right)}{(iw+\beta)\prod_{n=1}^{N}(1+\lambda_n(iw+\beta))} dw, \end{aligned} \tag{44}$$

where the first equality uses the channel transformation $\tilde{\mathbf{h}_{\text{N}}} = U_P^{\frac{H}{2}} \bar{\mathbf{h}}_{\text{N}}$ and the inner integral is computed by using Gaussian integral. In the second equality, λ_n is the nth eigenvalue determined by $\gamma_{\text{th}}(1-\rho)\sigma_{a\text{N}}^2 + \sigma_{c\text{N}}^2$. We now obtain the new equation $\Theta 1A$ provided in (21) using the residue theory and partial fraction expansion as in [53].

APPENDIX B

Proof of (26):

Using values of $Pr(\Gamma_{\text{N}}^{s_{\text{F}}})$ and $Pr(\Gamma_{\text{NF}})$ from (8) and (17), we obtain

$$\begin{aligned}&\Theta_{1C}(\gamma_{\text{th}}) \\ &= Pr\left(\frac{(1-\rho)p_{\text{F}}P_s||\tilde{\mathbf{h}}_{\text{N}}||^2_{\tilde{\mathbf{P}}_{\text{N}}}}{(1-\rho)p_{\text{N}}P_s||\tilde{\mathbf{h}}_{\text{N}}||^2_{\tilde{\mathbf{P}}_{\text{N}}} + (1-\rho)\sigma_{\text{N}}^2 \text{tr}(\tilde{\mathbf{r}}_{\text{N}}^H \mathbf{R}_{\text{N}j-Rx})} \right. \\ &\left. > \gamma_{\text{th}}, \frac{|h_{\text{NF}}|^2||\mathbf{h}_{\text{N}}||^2_{\tilde{\mathbf{P}}_{\text{N}}}\eta P_s(2\alpha+(1-\alpha)\rho)}{(\sigma_{\text{F}}^2+\sigma_{\text{NF}}^2)(1-\alpha)} < \gamma_{\text{th}}\right) \\ &= Pr\left(\frac{a_1||\tilde{\mathbf{h}}_{\text{N}}||^2_{\tilde{\mathbf{P}}_{\text{N}}}}{a_2||\tilde{\mathbf{h}}_{\text{N}}||^2_{\tilde{\mathbf{P}}_{\text{N}}}+1} > \gamma_{\text{th}}, c|h_{\text{NF}}|^2||\mathbf{h}_{\text{N}}||^2_{\tilde{\mathbf{P}}_{\text{N}}} < \gamma_{\text{th}}\right), \end{aligned} \tag{45}$$

the second equality is attained by considering that the beamformer vectors are linearly dependent, while $a_1 = \frac{(1-\rho)p_{\text{F}}P_s}{(1-\rho)\sigma_{\text{N}}^2 \text{tr}(\tilde{\mathbf{r}}_{\text{N}}^H \mathbf{R}_{\text{N}j-Rx})}$, $a_2 = \frac{(1-\rho)p_{\text{N}}P_s}{(1-\rho)\sigma_{\text{N}}^2 \text{tr}(\tilde{\mathbf{r}}_{\text{N}}^H \mathbf{R}_{\text{N}j-Rx})}$. We achieve the expression Θ_{1A} given in (26)

REFERENCES

[1] Z. Shi, W. Gao, S. Zhang, J. Liu, and N. Kato, "AI-enhanced cooperative spectrum sensing for non-orthogonal multiple access," *IEEE Wireless Commun.*, vol. 27, no. 2, pp. 173–179, Apr. 2020.

[2] L. Dai, B. Wang, Z. Ding, Z. Wang, S. Chen, and L. Hanzo, "A survey of non-orthogonal multiple access for 5G," *IEEE Commun. Surveys Tuts.*, vol. 20, no. 3, pp. 2294–2323, 3rd Quart., 2018.

[3] S. M. R. Islam, N. Avazov, O. A. Dobre, and K.-S. Kwak, "Power-domain non-orthogonal multiple access (NOMA) in 5G systems: Potentials and challenges," *IEEE Commun. Surveys Tuts.*, vol. 19, no. 2, pp. 721–742, 2nd Quart., 2017.

[4] J.-M. Kang, I.-M. Kim, and C.-J. Chun, "Deep learning-based MIMO-NOMA with imperfect SIC decoding," *IEEE Syst. J.*, vol. 14, no. 3, pp. 3414–3417, Sep. 2020.

[5] B. Kimy, S. Lim, H. Kim, S. Suh, J. Kwun, S. Choi, C. Lee, S. Lee, and D. Hong, "Non-orthogonal multiple access in a downlink multiuser beamforming system," in *Proc. IEEE Mil. Commun. Conf.*, Nov. 2013, pp. 1278–1283.

[6] Z. Yang, Z. Ding, P. Fan, and G. K. Karagiannidis, "On the performance of non-orthogonal multiple access systems with partial channel information," *IEEE Trans. Commun.*, vol. 64, no. 2, pp. 654–667, Feb. 2016.

[7] Z. Ding, P. Fan, and H. V. Poor, "Impact of user pairing on 5G nonorthogonal multiple-access downlink transmissions," *IEEE Trans. Veh. Technol.*, vol. 65, no. 8, pp. 6010–6023, Aug. 2016.

[8] S. Timotheou and I. Krikidis, "Fairness for non-orthogonal multiple access in 5G systems," *IEEE Signal Process. Lett.*, vol. 22, no. 10, pp. 1647–1651, Oct. 2015.

[9] J. Choi, "On the power allocation for a practical multiuser superposition scheme in NOMA systems," *IEEE Commun. Lett.*, vol. 20, no. 3, pp. 438–441, Mar. 2016.

[10] L. R. Varshney, "Transporting information and energy simultaneously," in *Proc. IEEE Int. Symp. Inf. Theory*, Jul. 2008, pp. 1612–1616.

[11] T. B. Doan and T. H. Nguyen, "Exploiting SWIPT for coordinated-NOMA systems under Nakagami-M fading," *IEEE Access*, vol. 12, pp. 19216–19228, 2024.

[12] E. Björnson, J. Hoydis, and L. Sanguinetti, "Massive MIMO has unlimited capacity," *IEEE Trans. Wireless Commun.*, vol. 17, no. 1, pp. 574–590, Jan. 2018.

[13] S. Asheer and S. Kumar, "A comprehensive review of cooperative MIMO WSN: Its challenges and the emerging technologies," *Wireless Netw.*, vol. 27, no. 2, pp. 1129–1152, Nov. 2020.

[14] P. Mursia, I. Atzeni, L. Cottatellucci, and D. Gesbert, "Enforcing statistical orthogonality in massive MIMO systems via covariance shaping," 2021, *arXiv:2106.07952*.

[15] J. Fang, X. Li, H. Li, and F. Gao, "Low-rank covariance-assisted downlink training and channel estimation for FDD massive MIMO systems," *IEEE Trans. Wireless Commun.*, vol. 16, no. 3, pp. 1935–1947, Mar. 2017.

[16] J. Nam, A. Adhikary, J.-Y. Ahn, and G. Caire, "Joint spatial division and multiplexing: Opportunistic beamforming, user grouping and simplified downlink scheduling," *IEEE J. Sel. Topics Signal Process.*, vol. 8, no. 5, pp. 876–890, Oct. 2014.

[17] H. Yin, D. Gesbert, M. Filippou, and Y. Liu, "A coordinated approach to channel estimation in large-scale multiple-antenna systems," *IEEE J. Sel. Areas Commun.*, vol. 31, no. 2, pp. 264–273, Feb. 2013.

[18] L. You, X. Gao, X.-G. Xia, N. Ma, and Y. Peng, "Pilot reuse for massive MIMO transmission over spatially correlated Rayleigh fading channels," *IEEE Trans. Wireless Commun.*, vol. 14, no. 6, pp. 3352–3366, Jun. 2015.

[19] R. H. Y. Perdana, T.-V. Nguyen, and B. An, "Adaptive user pairing in multi-IRS-aided massive MIMO-NOMA networks: Spectral efficiency maximization and deep learning design," *IEEE Trans. Commun.*, vol. 71, no. 7, pp. 4377–4390, Jul. 2023.

[20] A. Adhikary, J. Nam, J.-Y. Ahn, and G. Caire, "Joint spatial division and multiplexing—The large-scale array regime," *IEEE Trans. Inf. Theory*, vol. 59, no. 10, pp. 6441–6463, Oct. 2013.

[21] R. R. Müller, L. Cottatellucci, and M. Vehkaperä, "Blind pilot decontamination," *IEEE J. Sel. Topics Signal Process.*, vol. 8, no. 5, pp. 773–786, Oct. 2014.

[22] J. Nam, J.-Y. Ahn, A. Adhikary, and G. Caire, "Joint spatial division and multiplexing: Realizing massive MIMO gains with limited channel state information," in *Proc. 46th Annu. Conf. Inf. Sci. Syst. (CISS)*, Mar. 2012, pp. 1–6.

[23] A. Padmanabhan, A. Tölli, and I. Atzeni, "Distributed two-stage multi-cell precoding," in *Proc. IEEE 20th Int. Workshop Signal Process. Adv. Wireless Commun. (SPAWC)*, Jul. 2019, pp. 1–5.

[24] N. N. Moghadam, H. Shokri-Ghadikolaei, G. Fodor, M. Bengtsson, and C. Fischione, "Pilot precoding and combining in multiuser MIMO networks," *IEEE J. Sel. Areas Commun.*, vol. 35, no. 7, pp. 1632–1648, Jul. 2017.

[25] H. Yin, L. Cottatellucci, D. Gesbert, R. R. Muller, and G. He, "Robust pilot decontamination based on joint angle and power domain discrimination," *IEEE Trans. Signal Process.*, vol. 64, no. 11, pp. 2990–3003, Jun. 2016.

[26] M. Ghous, A. K. Hassan, Z. H. Abbas, and G. Abbas, "Modeling and analysis of self-interference impaired two-user cooperative MIMO-NOMA system," *Phys. Commun.*, vol. 48, Oct. 2021, Art. no. 101441.

[27] P. Mursia, I. Atzeni, D. Gesbert, and L. Cottatellucci, "Covariance shaping for massive MIMO systems," in *Proc. IEEE Global Commun. Conf. (GLOBECOM)*, Dec. 2018, pp. 1–6.

[28] C.-X. Wang, S. Wu, L. Bai, X. You, J. Wang, and I. Chih-Lin, "Recent advances and future challenges for massive MIMO channel measurements and models," *Sci. China Inf. Sci.*, vol. 59, no. 2, pp. 1–16, Jan. 2016.

[29] M. Lin, L. Yang, W.-P. Zhu, and M. Li, "An open-loop adaptive space-time transmit scheme for correlated fading channels," *IEEE J. Sel. Topics Signal Process.*, vol. 2, no. 2, pp. 147–158, Apr. 2008.
[30] Á. Pendás-Recondo, R. G. Ayestarán, and J. A. López-Fernández, "Beamforming for NOMA under similar channel conditions including near-field formulation," *IEEE Access*, vol. 11, pp. 71250–71259, 2023.
[31] Z. Ding, F. Adachi, and H. V. Poor, "The application of MIMO to non-orthogonal multiple access," *IEEE Trans. Wireless Commun.*, vol. 15, no. 1, pp. 537–552, Jan. 2016.
[32] T. N. Do, D. B. da Costa, T. Q. Duong, and B. An, "Improving the performance of cell-edge users in MISO-NOMA systems using TAS and SWIPT-based cooperative transmissions," *IEEE Trans. Green Commun. Netw.*, vol. 2, no. 1, pp. 49–62, Mar. 2018.
[33] Y. Yuan and Z. Ding, "The application of non-orthogonal multiple access in wireless powered communication networks," in *Proc. IEEE 17th Int. Workshop Signal Process. Adv. Wireless Commun. (SPAWC)*, Jul. 2016, pp. 1–5.
[34] L. Bing, Y. Gu, T. Aulin, and J. Wang, "Design of autoconfigurable random access NOMA for URLLC industrial IoT networking," *IEEE Trans. Ind. Informat.*, vol. 20, no. 1, pp. 190–200, Jan. 2024.
[35] D. C. González, D. B. da Costa, and J. C. S. Santos Filho, "Distributed TAS/MRC and TAS/SC schemes for fixed-gain AF systems with multiantenna relay: Outage performance," *IEEE Trans. Wireless Commun.*, vol. 15, no. 6, pp. 4380–4392, Jun. 2016.
[36] V. N. Q. Bao, T. Q. Duong, and C. Tellambura, "On the performance of cognitive underlay multihop networks with imperfect channel state information," *IEEE Trans. Commun.*, vol. 61, no. 12, pp. 4864–4873, Dec. 2013.
[37] J. So and Y. Sung, "Improving non-orthogonal multiple access by forming relaying broadcast channels," *IEEE Commun. Lett.*, vol. 20, no. 9, pp. 1816–1819, Sep. 2016.
[38] Z. Ding, Z. Yang, P. Fan, and H. V. Poor, "On the performance of non-orthogonal multiple access in 5G systems with randomly deployed users," *IEEE Signal Process. Lett.*, vol. 21, no. 12, pp. 1501–1505, Dec. 2014.
[39] J. Choi, "Effective capacity of NOMA and a suboptimal power control policy with delay QoS," *IEEE Trans. Commun.*, vol. 65, no. 4, pp. 1849–1858, Apr. 2017.
[40] Y. Zhang, H.-M. Wang, Q. Yang, and Z. Ding, "Secrecy sum rate maximization in non-orthogonal multiple access," *IEEE Commun. Lett.*, vol. 20, no. 5, pp. 930–933, May 2016.
[41] A. Goldsmith, *Wireless Communications*. Cambridge, U.K.: Cambridge Univ. Press, 2005.
[42] S. Gautam, E. Lagunas, S. K. Sharma, S. Chatzinotas, and B. Ottersten, "Relay selection strategies for SWIPT-enabled cooperative wireless systems," in *Proc. IEEE 28th Annu. Int. Symp. Pers., Indoor, Mobile Radio Commun. (PIMRC)*, Oct. 2017, pp. 1–7.
[43] V. Stankovic and M. Haardt, "Generalized design of multi-user MIMO precoding matrices," *IEEE Trans. Wireless Commun.*, vol. 7, no. 3, pp. 953–961, Jun. 2008.
[44] H. Sung, S.-R. Lee, and I. Lee, "Generalized channel inversion methods for multiuser MIMO systems," *IEEE Trans. Commun.*, vol. 57, no. 11, pp. 3489–3499, Nov. 2009.
[45] K. Zu, R. C. de Lamare, and M. Haardt, "Multi-branch tomlinson-harashima precoding design for MU-MIMO systems: Theory and algorithms," *IEEE Trans. Commun.*, vol. 62, no. 3, pp. 939–951, Mar. 2014.
[46] S. G. Hong and S. Bahk, "Performance analysis and fairness maximization in NOMA systems with improper Gaussian signaling under imperfect successive interference cancellation," *IEEE Access*, vol. 8, pp. 50439–50451, 2020.
[47] H. Cheng, Y. Xia, Y. Huang, and L. Yang, "Improper Gaussian signaling for downlink NOMA systems with imperfect successive interference cancellation," *IEEE Trans. Wireless Commun.*, vol. 21, no. 9, pp. 7753–7763, Sep. 2022.
[48] H.-T. Chiu and F. Maehara, "Improper Gaussian signaling for two-user MISO-NOMA systems considering hardware impairments and imperfect SIC," *IEEE Access*, vol. 11, pp. 59827–59839, 2023.
[49] S. Menaa, A. Khelil, K. M. Rabie, X. Li, and G. Nauryzbayev, "On the ergodic capacity of MIMO-NOMA systems with JTRAS protocol under imperfect SIC and CSI," *Int. J. Electron.*, vol. 1, pp. 1–20, Aug. 2023.
[50] H. Sampath, P. Stoica, and A. Paulraj, "Generalized linear precoder and decoder design for MIMO channels using the weighted MMSE criterion," *IEEE Trans. Commun.*, vol. 49, no. 12, pp. 2198–2206, May 2001.
[51] S. Kaviani, O. Simeone, W. A. Krzymien, and S. S. Shitz, "Linear precoding and equalization for network MIMO with partial cooperation," *IEEE Trans. Veh. Technol.*, vol. 61, no. 5, pp. 2083–2096, Jun. 2012.
[52] S. Kaviani and W. A. Krzymien, "Robust joint precoder and equalizer design in MIMO communication systems," in *Proc. IEEE Wireless Commun. Netw. Conf. (WCNC)*, Apr. 2012, pp. 277–282.
[53] Q. Sun, Y. Wu, X. Chen, and J. Zhang, "SLNR-based joint RIS-UE association and beamforming design for multi-RIS aided wireless communications," *IEEE Trans. Veh. Technol.*, vol. 73, no. 6, pp. 8660–8670, Jun. 2024.

ZAIN UL ABIDIN JAFFRI received the M.E. degree in electronics and communication engineering and the Ph.D. degree in communication and information systems from Chongqing University, China. He is currently an Associate Professor with the School of International Education, Xiamen University of Technology, Xiamen, China. His main research interests include wireless sensor networks, antenna design and propagation, mobile and wireless communication networks, and advanced computer networks.

MUHAMMAD FAHEEM (Member, IEEE) received the B.Sc. degree in computer engineering from the Department of Computer Engineering, University College of Engineering and Technology, Bahauddin Zakariya University, Multan, Pakistan, in 2010, the M.S. degree in computer science from the Faculty of Computer Science and Information System, Universiti Teknologi Malaysia, Malaysia, in 2012, and the Ph.D. degree from the Faculty of Computing, School of Computer Science, Universiti Teknologi Malaysia in 2021. In the past, he was a Lecturer with the COMSATS Institute of Information and Technology, Pakistan, from 2011 to 2012. Before his current role, he held a Lecturer position at the Comsats Institute of Information and Technology, Pakistan, from 2012 to 2014. Subsequently, he furthered his academic career as an Assistant Professor at the Department of Computer Engineering, Abdullah Gul University, Turkey, where he contributed from 2014 until 2022. Presently, he is working as an Assistant Professor with the Department of Computing Science, School of Technology and Innovations, University of Vaasa, Finland. His research ambitiously spans several cutting-edge domains, including cybersecurity, blockchain technology, artificial intelligence, smart grids, and smart cities. His academic contributions are significant, with numerous papers published in well-respected, peer-reviewed journals and conferences. Furthermore, he has been an active reviewer for a wide array of prestigious journals associated with IEEE, Elsevier, Springer, Wiley, and MDPI, showcasing his dedication to advancing knowledge and technology in his field.